Genetic Dissection Uncovers Genome Wide Marker-Trait Associations for Plant Growth, Yield and Yield Related Traits Under Varying Nitrogen Levels in Nested Synthetic Wheat Introgression Libraries

NITIKA SANDHU
Punjab Agricultural University
Amandeep Kaur
Punjab Agricultural University
Mehak Sethi
Punjab Agricultural University
Satinder Kaur
Punjab Agricultural University
Varinderpal Singh
Punjab Agricultural University
Achla Sharma
Punjab Agricultural University
Alison R Bentley
CIMMYT: Centro Internacional de Mejoramiento de Maiz y Trigo
Tina Barsby
NIAB: National Institute of Agricultural Botany
Parveen Chhuneja (pchhuneja@pau.edu)
Punjab Agricultural University https://orcid.org/0000-0002-8599-9479

Research Article

Keywords: nitrogen, genome wide association studies, marker-trait association, wheat, yield

Posted Date: June 9th, 2021

DOI: https://doi.org/10.21203/rs.3.rs-582649/v1

Genetic dissection uncovers genome wide marker-trait associations for plant growth, yield and yield related traits under varying nitrogen levels in nested synthetic wheat introgression libraries

Nitika Sandhu[1], Amandeep Kaur[1], Mehak Sethi[1], Satinder Kaur[1], Varinderpal-Singh[2], Achla Sharma[3], Alison R Bentley[4,5], Tina-Barsby[4], Parveen Chhuneja[1#]

1. School of Agricultural Biotechnology, Punjab Agricultural University, Ludhiana-141004. Punjab, India
2. Department of Soils, Punjab Agricultural University, Ludhiana-141004. Punjab, India
3. Department of Plant Breeding and Genetics, Punjab Agricultural University, Ludhiana-141004. Punjab, India
4. National Institute of Agricultural Botany, Cambridge, UK
5. Present Address: International Wheat and Maize Improvement Center (CIMMYT), El Batan, Mexico

[#]corresponding author: pchhuneja@pau.edu; orcid ID: 0000-0002-8599-9479

Key message

To meet future wheat production demands, improving nitrogen use while maintaining grain yield is vital. We identified marker-trait associations affecting plant growth, yield and yield related traits under varying nitrogen levels. We also identified promising breeding lines with significant genetic variations and carrying the trait-associated markers or candidate genes. These may serve as potential donors to be exploited further in genomics-assisted breeding programs targeting improved NUE while maintaining grain yield in wheat.

Abstract

Nitrogen is one of the most important macronutrients for crop growth and metabolism. To identify marker-trait associations for complex NUE-related agronomic traits, field experiments were conducted on nested synthetic wheat introgression libraries at three nitrogen input levels across two seasons. The introgression libraries were genotyped using the 35K Axiom® Wheat Breeder's Array and genetic diversity and population structure were examined. Significant phenotypic variation was observed across genotypes, treatments and their interactions across seasons for all the 22 traits measured. Significant positive correlations were observed among grain yield and yield attributing traits and root traits. Across seasons, a total of 233 marker-trait associations (MTAs) associated with fifteen traits of interest at differential levels of nitrogen (N0, N60 and N120) were detected using 9,474 genome-wide single nucleotide polymorphism (SNP) markers. Of these, 45 MTAs for 10 traits in the N0 treatment, 100 MTAs for 11 traits in the N60 treatment and 88 MTAs for 11 traits in the N120 treatment were detected. We identified putative candidate genes underlying the significant MTAs which were associated directly or indirectly with various biological processes, cellular component organization and molecular functions involving improved plant growth and grain yield. In addition, the top 10 lines based on N response and grain yield across seasons and treatments were identified. The identification and introgression of superior alleles/donors improving NUE while maintaining grain yield may open new avenues in designing next-generation nitrogen efficient high yielding wheat varieties.

Keywords: nitrogen, genome wide association studies, marker-trait association, wheat, yield

Introduction

The global demand for nitrogen currently stands at about 117 million metric tons with a projected annual increase of approximately 1.5% expected in the near future (FAO 2019). Farmers generally apply high doses of nitrogenous fertilizers to ensure good yields. The high input of commercially available fertilizers has led to the degradation of air, soil, and water quality (Hickman et al. 2014; Russo et al. 2017). In addition, when the supply of nitrogen is in excess of crop nitrogen demand, it increases the susceptibility of plants to various diseases and insect pests (Reddy 2017). Therefore, it is necessary to optimize and improve the nitrogen use efficiency (NUE) of cereal crops to maximize yield in addition to minimizing the negative impact of increase in nitrogen use on the environments and natural resources. Identification of marker-trait associations can be used to make effective targeted introgressions and is one possible genetic method to address the challenge of developing nitrogen efficient wheat varieties with stable yield under nitrogen limited environments.

Wheat varieties that maintain yield under moderate or intense nitrogen deficiency can adapt to low input systems. To breed such varieties, genetic variation for adaptation traits to nitrogen deficiency is required. To date, limited quantitative trait loci (QTL) for both yield and its response to N deficiency in wheat under field conditions have been documented. Detection of genotypes and underlying QTLs for maintaining yields at low nitrogen levels are of value in wheat breeding programs designed to increase nitrogen-deficiency tolerance. Some QTLs influencing nitrogen uptake have been genetically mapped in wheat under different doses of fertilizer application using bi-parental populations (An et al. 2006; Laperche et al. 2007; Xu et al. 2014; Deng et al. 2017; Mahjourimajd et al. 2016). A number of genetic loci for agronomic traits related to nitrogen use and grain yield have also been mapped to the chromosomal regions containing the *GS2* gene in wheat and rice (Prasad et al. 1999; Obara et al. 2001; Yamaya et al. 2002; Fontaine et al. 2009; Habash et al. 2006; Laperche et al. 2007). This suggests the role of the genomic region surrounding *GS2* is favourable in breeding wheat and rice varieties with improved agronomic performance and nutrient use efficiency. Other genetic regions associated with nutrient uptake have also been detected in rice (Wissuwa et al. 1998; Ming et al. 2000), wheat (Su et al. 2006; 2009), maize (Zhu et al. 2005), common bean (Liao et al. 2004; Yan et al. 2004), and soybean (Li et al. 2005; Liang et al. 2010). The *NRT2.1*, *NRT2.2*, and *NAR2.1* gene have been reported to be the important contributors to the high affinity transport system in *Arabidopsis* roots (Orsel et al. 2006). Sixteen genes were identified in wheat homologous to characterized *Arabidopsis* low-affinity nitrate transporter NPF genes,

suggesting a complex wheat NPF gene family (Buchner and Hawkesford 2014). The regulation of wheat NFP genes by plant N-status indicated involvement of these transporters in substrate transport in relation to N-metabolism.

The phenotypic traits reported to be associated with NUE in cereal crop so far include root number, length, density and branching (Morita et al. 1988; Yang et al. 2012; Steffens and Rasmussen 2016), dense and erect panicle (Sun et al. 2014), plant height (Gaju et al. 2011), and leaf width (Zhu et al. 2020). The colocation of QTLs for N-uptake and root architecture traits have suggested that breeding for better and efficient root systems is a way to improve NUE (Coque et al. 2008; Sandhu et al. 2015).

Diverse accessions, landraces, breeding populations, and next-generation mapping populations, including nested-association mapping (NAM) and multi-parent advanced generation inter-cross (MAGIC) populations have shown potential for mining novel genetic variation in rice (Zhao et al. 2011; Subedi et al. 2019; Sandhu et al. 2019), wheat (Mackay et al. 2014), maize (Yu et al. 2008) and soybean (Xavier et al. 2015). NAM and MAGIC populations have proven advantageous over biparental populations as they capture additional recombination breakpoints thus increasing the allelic diversity and improving the power of QTL detection (Yu et al. 2008; Scott et al. 2020). Further, the availability of high throughput genotyping platforms to generate uniformly distributed genome wide molecular markers are critical for the high-resolution genetic dissection of polygenic traits, and the tracking of favourable alleles in breeding populations (Pandey et al. 2012; Varshney et al. 2013; Pandey et al. 2016). To date, a series of high-density wheat SNP arrays such as the Illumina 9K iSelect SNP array (Cavanagh et al. 2013), Illumina 90K iSelect SNP genotyping array (Wang et al. 2014), 15K SNP array (Boeven et al. 2016), Axiom® 660K SNP array, 55K SNP array, Axiom® HD 820K genotyping array (Winfield et al. 2016), 35K Axiom array (Allen et al. 2017) and 50K Triticum TraitBreed array (Rasheed and Xia 2019) have been developed and their utility has been demonstrated across a range of applications.

In the present study we developed nested synthetic wheat introgression libraries capturing novel genetic variation. The libraries were genotyped using a high-density SNP array and phenotypically assessed for root traits and agronomic performance under three nitrogen input conditions in the field. Genome-wide association mapping was used to identify marker-trait

associations for the root and agronomic traits and lines carrying favourable genetic combinations were also identified for use in future breeding for improved nitrogen use.

Material and Methods

Plant material

A total of 31 cultivated and 12 synthetic wheats were evaluated at 6 nitrogen levels (N0, N40, N80, N120, N160 and N200) in 3 replications in 2016-2017 and 2017-2018 during the rabi seasons at Punjab Agricultural University, Ludhiana, India. The synthetic wheats PDW233/*Ae. tauschii* acc. pau 14135 and PBW114/*Ae. tauschii* acc. pau 14170 produced high grain yields as well as high agronomic efficiency at low fertilizer N doses (unpublished data). These synthetic wheats were used to develop a nested synthetic hexaploid wheat (N-SHW) introgression library constituting a set of 352 lines derived from four sub-populations. The N-SHW library was made up of subsets from four populations (Pop1: 75 lines from PDW233/*Ae. tauschii* acc. pau 14135 amphiploid //2*BWL4444; Pop2: 106 lines from PDW233/*Ae. tauschii* acc. pau 14135 amphiploid //2*BWL3531; Pop3: 88 lines from PBW114/*Ae. tauschii* acc. pau 14170 amphiploid //2*BWL4444; Pop4: 83 lines from PBW114/*Ae. tauschii* acc. pau 14170 amphiploid //2*BWL3531 along with the two common parents (BWL3531, BWL4444) and other unique parents (PDW233, PBW114, *Ae. tauschii* acc. pau 14135 amphiploid and *Ae. tauschii* acc. pau 14170 amphiploid). The breeding scheme used to develop the N-SHW introgression library is summarised in Fig. 1.

Agronomic practices and management of experiments

The N-SHW library, six parents and two synthetic hexaploid wheats were assessed at the experimental farms of School of Agricultural Biotechnology, PAU Ludhiana (30˚ 54' N latitude, 75˚48' E longitude, and 247 m above sea level) over 2 years in 3 nitrogen level (6-year x N combinations). Details of the number of lines tested and experimental design is provided in Table 1. The breeding material was sown on 21th of November and 18th of November in 2018 and 2019, respectively. In both years the experiments were conducted at three nitrogen levels [i.e. zero N (0 Kg ha^{-1}), half N (60 Kg ha^{-1}) and full N (recommended, 120 Kg ha^{-1}),] referred to as N0, N1 and N2, respectively. The recommended dose of phosphorus, potassium and manganese was applied at the time of sowing. Half of the nitrogen (N) was applied at the time of sowing while the other half was applied in two equal splits, the first at crown root initiation stage and the remaining at the maximum tillering stage in both the

N1 and N2 experiments. N0 was treated as a control. Recommended fungicides and insecticides were applied to control stripe rusts, brown rusts, and aphids at jointing, booting and 10 days after anthesis to prevent diseases and pests. Weeds were controlled manually.

Characterization of phenotypic traits

A total of twenty-two traits were assessed in all experiments across both seasons except the maximum root length and root angle which were measured in 2018 only. The details of the NUE related traits, root and plant morphological traits, grain yield and yield attributing traits are presented in Supplementary Fig. S1. Destructive sampling of six plants per plot was done at 60 DAS to evaluate early root and shoot traits (Supplementary Fig. S2). Shoots were separated from the roots, fresh root weight (FRW; g) and fresh shoot weight (FSW; g) were measured. The root and shoot samples were dried at 70°C in an oven until constant shoot dry weight (g) was observed, while the roots were cleaned thoroughly and stored in 70% alcohol at 4 °C for root trait evaluation. MRL (maximum root length) and RA (root angle) were measured using ImageJ software. TRL (total root length), RSA (total root surface area), RD (total root diameter), RV (total root volume), NF (number of forks) and Ntips (number of tips) were recorded using WinRhizo STD4800 (Supplementary Fig. S2). The roots were then dried at 70°C in the oven until constant RDW was observed. The data on nitrogen uptake related traits was recorded using chlorophyll meter (SPAD502) and leaf color chart (LCC). The LCC provides a decision support system to the farmers for sustaining the high yields with optimum nitrogen dose in the field crops. It measures the leaf color variations of 6 SPAD (Soil Plant Analysis Development Meter) units comprising 3, 3.5, 4.0, 4.5, 5.0 and 6.0 and provides nitrogen recommendation in the field crops. Flag leaf length (FLL) and flag leaf width (FLW) were recorded using a centimeter scale. Days to 50% flowering (DTF) was recorded when 50% of the plants in a plot exerted their panicles. Spikelets per spike (SPS) was counted manually from five random plants. NPT (number of productive tillers) was counted manually in 0.5 m row length and SB (shoot biomass) at harvesting was measured from 0.5 m row length. PHT (plant height) in cm was measured as the mean height of five random plants for each entry measured from the base of the plant to the tip of the panicle during maturity stage. The plants were harvested at physiological maturity or when 80-85% of the panicles turned to golden yellow and the panicles at the base were already at the hard dough stage; harvested grains were threshed, dried and weighed to determine the GY (grain yield).

Phenotypic data analysis

Analysis of variance (ANOVA), experiment and experiment-wise mean for each season was calculated using mixed model analysis in PBTools V 1.4.0. for augmented design and in STAR Version: 2.0.1 for the split plot design. In split plot design the nitrogen levels were considered as the main plot and the breeding lines as subplot. Fisher's t-test was used to determine the significant difference among the breeding lines, treatments and to estimate the interactions. The correlation analysis among traits was performed in R. v.1.1.423

To evaluate the phenotypic stability and grain yield adaptability of the breeding lines across seasons and treatments, the GGE biplot analysis was performed, considering the effects of genotype (G) and genotype by environment (GE) as random. The best linear unbiased prediction (BLUP) values of the G and GE effects were calculated. The multiplicative model in PB tool version 1.3 (bbi.irri.orgbbi.irri.org) was used to explain the relationship between genotype and seasons.

Genotypic data

High-density genotyping was performed using the 35K Axiom® Wheat Breeder's Array (Affymetrix UK Ltd., United Kingdom). The quality pre-processing of 35,143 markers obtained from the 35K chip was done using PLINK software (Purcell et al. 2007). A total of 9,474 SNPs with MAF (minor allele frequency) of >5%, maximum heterozygote proportion of 0.1 and missing rates < 0.1 were used to estimate genetic relationships and for the mapping of marker-trait associations for different traits associated with plant growth, yield and yield related traits. APCA was carried out to detect and correct for population structure.

Population structure and association analysis

The model-based STRUCTURE V. 2.3.4 software was used to test *K* values from 1 to 10, with a burn-in period to 10,000 and 1,000,000 MCMC reps after burn-in in order to assess population structure in the 352 breeding lines using a total of 9,474 SNPs. The consistency and accuracy of the results was validated across 10 runs for each *K*. The *K* value with maximum likelihood over the 10 runs was used to estimate the most appropriate number of clusters (Pritchard and Wen 2004). The population structure was determined by plotting the proposed number of subpopulations against the delta *k* (Earl and Vonholdt 2012). Principal components analysis (PCA) was performed in R/GAPIT and added iteratively to the fixed model, ranging from PC1 to PC10.

Significant marker-trait associations were identified using CMLM (compressed mixed linear model)/P3D (population parameters previously defined) in GAPIT (Genome Association and Prediction Integrated Tool) executed in R. Identity by state (IBS) values and a relatedness matrix were used to estimate the random effect and genetic similarity of the accessions, respectively. The statistical power of the association studies was further improved by considering the population structure (*Q* value) and kinship matrix (*K*) estimated from the genotyping data. The Bonferroni correction method was used to correct for false positives in the analysis, using the stringent p-value benchmark. The Bonferroni multiple test correction was performed (0.05/9474; significance level of 5%/total number of markers used in analysis) and the calculated threshold value was 5.28×10^{-6}. The allelic effect of all the significant markers associated with the measured traits was determined by comparing the mean phenotypic values and the significant allelic variants for the trait/s using a Kruskal–Wallis test in R.

Candidate gene analysis and functional annotation of putative candidate genes

SNPs that exhibited a false discovery ratio (FDR) corrected p-value <0.05 for a particular trait of interest were evaluated as markers for the potential putative candidate genes. A window of 1Mb adjacent to each significant SNP was examined for candidate genes and annotations were identified through the Ensembplants database (http://plants.ensembl.org/index.html).

The functional annotation and gene ontology of identified putative candidate genes was performed using OMIX box software. Blast (E-value$\leq 10^{-5}$) was performed using the CloudBlast tool against *Triticum* (nr_subset)[monocots_*triticum*, taxa:4564] and NCBI non-redundant database (http://www.ncbi.nlm.nih.gov), followed by the InterPro using CloudIPS, followed by GO mapping (Gene Ontology), and annotation configuration. GO terms were then used to generate the semantic similarity-based scatterplots/interactive graphs/tag clouds by using REVIGO (http://revigo.irb.hr/).

Defining N-insensitive and N-sensitive lines

The genotypes that showed more or equal/stable grain yield with the minimal application of nitrogen fertilizer when compared to the recommended or standard nitrogen fertilizer application, were considered as the nitrogen insensitive genotypes (NIS) or the top grain yielders across seasons and treatments. On the other way around, the genotypes that were low yielding or not able to maintain the grain yield with the minimal application of nitrogen

fertilizer when compared to the recommended or standard nitrogen fertilizer application, were considered as the nitrogen sensitive genotypes (NS) or the poor grain yielders across seasons and treatments.

Results

Significant phenotypic trait variation and correlations detected across nitrogen treatments

The 352 N-SHW lines, six parents and two synthetic hexaploid wheat donors were screened for twenty-two traits in six growing conditions (2 years x 3 nitrogen level). Analysis of variance (ANOVA) revealed significant genetic variation for the root, plant morphological and agronomic traits among genotypes, treatments, seasons and their interactions (genotype x treatment, genotype x season, treatment x season and genotype x treatment x season) (Table 2). The detailed information on trial means, LSD and heritability for all the traits measured are presented in Supplementary Table S1. The results revealed significant genetic variations across genotypes, treatments and interactions in 2018-2019 and 2019-2020 seasons for all the traits measured (Supplementary Table S2). The phenotypic data of the traits measured in the present study were averaged across two seasons and are presented as mean values in Supplementary Table S3.

GY increased with applied N level. In the N0 treatment, the average GY of the tested breeding lines across seasons was 2022 kg ha^{-1} and ranged from 564 to 4092 kg ha^{-1} (Supplementary Table S3). In the N60 treatment, the GY varied from 882 to 4685 kg ha^{-1} with average GY of 2357 kg ha^{-1} and, while in N120 treatment, the GY varied from 1332 to 4270 with an average of 2579 kg ha^{-1} (Supplementary Table S3). Across seasons, N in the limited conditions (N0) resulted in the 14% and 22% GY reduction compared to N60 and N120 treatments, respectively. The N application also significantly increased the SB by 8% in N60 and 52% in N120 treatment across seasons. The average NPT across experiments was higher in N120 (28) compared to N60 (24) and N0 (22) (Supplementary Table S3). Under the N0 treatment, the average LCC value varied from 3.3 - 4.8, and ranged from 3.5 - 5.1 in the N60 treatment and from 4.1 - 5.3 in the N120 treatment (Supplementary Table S3). The response of lines in terms of average DSW across seasons increased from 3.28 in N0 to 3.62 in N60 to 3.75 in N120 treatment (Supplementary Table S3). The minimum and maximum value of DRW under N0 were 0.187 g and 2.425 g; 0.298 g and 2.001 g under N60 and 0.338 g and 2.333 g under N120,

respectively (Supplementary Table S3). The average root diameter was highest under N60 (0.610 g) compared to N0 (0.560 g) and N120 (0.409 g) (Supplementary Table S3). Across seasons, average flowering was delayed by 2 days under the N0 treatment compared to the N60 and N120 treatments. Average PHT was lower (92 cm) in N0 compared to N60 (95 cm) and N120 (99 cm).

We calculated the Pearson's correlation coefficients between all the traits measured in N0 (Fig. 2A), N60 (Fig. 2B) and N120 (Fig. 2C) treatments. The Pearson correlation coefficients across all treatments considering pooled mean data for all traits measured in the present study is presented in Supplementary Fig. S3. The strongest and most significant positive correlation among grain yield and yield attributing traits and root traits were observed in N60 treatment. The grain yield was significantly and positively correlated with SB ($r = 0.23$, $p < 0.001$), NPT ($r = 0.18$, $p < 0.01$), FRW ($r = 0.16$, $p < 0.01$), FSW ($r = 0.24$, $p < 0.001$), DSW ($r = 0.23$, $p < 0.001$) and with RSA = ($r = 0.23$, $p < 0.001$). Across treatments GY showed negative correlation with DTF, SB showed positive correlation with GY.

Population structure analysis detected three genetic sub-populations

The population structure of the N-SHW lines was assessed to understand the genetic structure of the 352 lines based on 9,474 SNPs distributed across all 21 wheat chromosomes. The most appropriate K explaining the population structure was K=3 at MAF $\geq$ 5% (Fig. 3A). The kinship heatmap indicated a weak relatedness in the panel (Fig. 3B). The first three principal components (PCs) were most informative gradually decreasing (Fig. 3C, Fig. 3D) until the tenth PC. The kinship and PCs were considered during the GWAS analysis to correct for population structure. The appropriate number of sub-populations was determined from the largest *delta K* value of 3 (Fig. 3E).

Mapping reveals significant marker-trait associations for all traits

GWAS was performed exploiting the phenotypic variability in the 352 N-SHW lines using 9,474 SNPs from the 35K Axiom® Wheat Breeder's Array. Using the -log(P) $\geq$0.001 at 5% significance level, a total of 233 marker-trait associations (MTAs) were detected across seasons associated with fifteen traits of interest at differential N levels (N0, N60 and N120; Table 3). Of these, 45 MTAs for the 10 traits in the N0 treatment, 100 MTAs were associated with 11 traits in the N60 treatment and 88 MTAs were associated with 11 traits in the N120 treatment

(Table 3). Across seasons and nitrogen treatments, a total of 53 MTAs associated with more than one trait/treatment were detected (Table 3). In addition to these 53 MTAs, another 41 MTAs associated with single trait only were detected across seasons (Supplementary Table S4). All MTAs detected in the present study either in one season, both seasons, each treatment or across treatments are compiled in Supplementary Table S5. Mapping detected MTAs on all subgenomes (A: 42, B: 18 and D: 34) across seasons and treatments. The highest number of MTAs were detected on chromosome 6A (26) followed by 2D (25), 3B (12), 4A (9), 6D (8), 2A (6), 2B (4) with 1 MTA on each of 1B, 4B, 5A and 7D. Considering all assessed traits, significant MTAs were reported for FRW (2A, 2D), FSW (2A, 2B, 2D, 5A, 7A), DRW (2A, 2B, 2D, 7A), DSW (2A, 2B, 2D), FLW (4A, 4B), NT (3A), SPS (1B), DTF (3A, 3B, 6A), SB (6A), TRL (6D), RSA (6A, 6D), RV (6D), tips (6A, 6D) and forks (6A, 6D).

The Manhattan plots depicting the significant -log (p-values) for the MTAs associated with NUE-related traits, root traits and yield/yield related traits measured in the present study at differential level of N are presented in Supplementary Fig. S4, Supplementary Fig. S5 and Fig. 4, respectively. Location of significant MTAs and SNP marker density distributed across 21 wheat chromosomes is presented in Fig. 5. The SNPs for positively correlated traits such as GY, BY, tips, RSA, RV and forks appeared to be collocated on chr 6A at differential level of N (Table 3). A genomic region on 2D (ranging from 576749639 - 702726797 bp) contained 25 detected MTAs for a range of traits (FRW, DRW, FSW and DSW) across seasons and treatments (Table 3; Fig. 5). A cluster of 17 SNPs spanning a 7.7 Mb region on the short arm of 6A showed association with GY at N60 and N120 (Fig. 5). Across seasons and treatments, significant association in a 198 kb region on the long arm of chr 6A were detected for root traits (RSA, RV, tips and forks). The SNP, AX-94565231 at 683.64 Mb on the long arm of chr 6D showed association with different root traits (RSA, RV, tips and forks) across seasons and treatments. In the N60 treatment, significant associations for FLW were detected in a 5.6 Mb region (549799824 - 544201748 bp) on the long arm of 4A. Interestingly, the association of the trait DTF with SNP AX-95136655 on chr 3B at 234.49 Mb was common under N0, N60 and N120 treatments (Fig. 5). In the N0 treatment, significant associations harbouring three strongly associated SNPs (AX-94593608, AX-94786978 and AX-95134564) spanning the genomic region 76 bp on the long arm of 3A were detected for NPT (Table 3). Further, single SNPs were identified in association with different traits at different N levels. For example, the SNP AX-94914391 (36.43 Mb, 6A) was significantly associated with SB at N0 and with GY

at both N60 and N120 (Fig. 5). The SNP AX-94705680 (598.80 Mb, 2B) showed association with FSW at N60 and with DRW at N120.

Candidate gene identification and functional annotation

In order to identify candidate genes underlying the consistent MTAs, we surveyed putative candidates in a 1Mb upstream and 1 Mb downstream region the identified significant SNPs using EnsemblPlants (http://plants.ensembl.org/index.html). Detailed information on the identified candidate genes is presented in Table 3.

The GO term of identified putative candidate genes were categorised into four groups according to their trait relatedness; NUE uptake related (LCC, SPAD, FSW, DSW), root morphological (MRL, TRL, RSA, RD, RV, NF, Ntips, FRW, DRW), plant morphological (FLL, FLW, PHT) and grain yield/yield attributing traits (DTF, S/S, NPT, SB, GY). Most of the putative candidate genes in NUE uptake related traits across treatments were associated with protein phosphorylation/proteolysis, recognition of pollen, molybdoprotein cofactor biosynthetic process, and transmembrane transport (Supplementary Table S6). Some were part of the cellular component organization and molecular functions of binding molecules and ions, catalytic activity, peptidase activity and transmembrane transport activity (Supplementary Table S6; Supplementary Fig. S6). The putative candidate genes for the root morphological traits were associated with nitrogen compound metabolic processes, phosphorylation, proteolysis, catabolic processes, response to stresses, regulation of flower development by delineating the composition and architecture of gene regulatory network underlying flower development, and carbohydrate metabolism (Supplementary Table S6 4; Supplementary Fig. S7). The cellular components include chloroplast, ribosome, membrane, cytoplasm, nucleus and mitochondria (Supplementary Table S6; Supplementary Fig. S7). The primary molecular functions related to these genes were catalytic activity (protease, peptidase, hydrolase, transferase, ligase, and oxidoreductase), and binding activity (small molecule binding, ion binding, lipid binding, and carbohydrate derivative binding) (Supplementary Table S6; Supplementary Fig. S7). The putative candidate genes for the plant morphological traits were mainly associated with phosphorylation, response to light-intensity, stress-related responses, and metabolic processes. They were related to the molecular functions of metal ion binding, catalytic activity, kinase activity, and DNA/RNA/ATP binding (Supplementary Table S6; Supplementary Fig. S8). The yield and yield attributing traits related putative candidate genes were associated with phosphorylation, metabolic process, protein folding, catabolic process, response to water-stress and light, flower development and pollen

recognition (Supplementary Table S6; Supplementary Fig. S8). The molecular functions include catalytic activity (peptidase, hydrolase, lyase, oxidoreductase, transferase), binding activity (ion, metal, ATP/GTP, polysaccharide, protein, DNA) and metabolic activity (Supplementary Table S6; Supplementary Fig. S9).

Selection of promising lines with stable performance for use in breeding

To identify stable breeding lines across treatments and seasons, a GGE biplot method was used. The first two PCs (principal components) explained 77.7% (PC1=50.3%, PC2=27.4%) of the total GGE variation in the data (Fig. 6). The ranking of breeding lines based on their mean GY and stability across seasons and treatments (Supplementary Table S7) was used to identify 20 breeding lines with high and stable yield across seasons and treatments (Supplementary Table S8; Fig. 7). Based on GY data across seasons and treatments, the top 10 N-insensitive (NIS-top grain yielders) and 10 N-sensitive (NS-poor grain yielders) breeding lines were identified (Table 4).

Further analysis was undertaken to assess the significant differences between the mean values of the allelic classes of MTAs for root growth and grain yield using the Kruskal–Wallis test. The presence of favourable alleles with significant differences was checked in promising breeding lines. This allowed the selection of 20 promising breeding lines possessing the favourable allele combinations for improving plant root growth (Fig. 8A) and grain yield under N limitation (Fig. 8B).

Discussion

Increase in crop production by development of high-yielding varieties is largely dependent on the supply of N fertilizers. Excessive application of nitrogenous fertilizer is becoming very expensive which accounts for the great loss of economic profit to the farmers in addition to the negative impacts on the environment (Hawkesford and Griffiths 2019). The reliable phenotyping under low nitrogen input is very challenging and affected by genotype (G), environment (E), and the G x E interactions (Rao et al. 2018). Proper understanding of the genotype behaviour, identification and development of nitrogen efficient genotypes without compromising the GY is a paramount need for improving the NUE. Notably, very few wheat breeding programs are targeting the development of nitrogen efficient genotypes. In crop plants such as wheat, the efforts are constrained due to the lack of variation in the cultivated germplasm for NUE. The narrow genetic diversity and fewer recombination events in the biparental mapping populations

may result in poor QTL detection power (Gangurde et al. 2019). The next generation high-resolution mapping populations such as nested synthetic wheat introgression libraries used in the present study may provide a vast and untapped source of genetic variations for the nitrogen use efficiency related traits due to high numbers of recombination events. The use of synthetic hexaploid wheat in the present study presenting an effective genetic resource for transferring the agronomically important genes from wild relatives to the common wheat (Li et al. 2018). The introgression of favourable alleles associated with root traits and grain yield from *Ae. tauschii* wild accessions to cultivated wheat (Fig. 8) indicated the potential of synthetic wheat providing new sources for improving yield potential and nutrient-use efficiency when bred with the modern wheat varieties.

The different traits associated with nitrogen uptake and nitrogen use efficiency were studied in nested synthetic wheat introgression libraries at three different nitrogen levels. The ANOVA results revealed the native variation across the genotypes toward the nitrogen response which had given the possibility to identify the nitrogen use efficient lines under differential levels of nitrogen. The genotypic variations purely reveal the phenotypic plasticity of the breeding lines toward traits. The diverse responses have been observed among the breeding lines across different level of nitrogen, despite similar growth conditions and an equal amount of nitrogenous fertilizer application in a given N level as indicated by significant differences among the genotypes within and across treatments and non-significant differences among the replications. Significant G x E, G x S, G x E, G x T x S interactions indicated that the seasons and environments under different level of N application was a critical factor in explaining the genotypic variance for the traits measured in the present study. The results reported in the present study concurred with other reported studies in rice (Srikanth et al. 2016) and wheat (Sial et al. 2005; Belete et al. 2018).

In general, the increase in GY was correlated with the increase in the rate of N fertilizer application, which might be due to availability of sufficient nitrogen for proper growth and development of the plants. Šarčević et al. (2014) reported 10% reduction of GY at low N condition compared to normal condition in wheat. The significant and positive correlation among different root traits and GY and yield attributing traits indicated complementary functional roles of the root traits in improving grain yield by improving nutrient acquisition from the soil. The collocation of MTAs for the correlated traits strengthens the significance of MTAs. A significant positive correlation between GY and NUE related traits in wheat, maize and oilseed

rape (He et al. 2017; Belete et al. 2018; Fageria et al. 2010) signified the importance of NUE related traits in improving GY under limited N conditions.

Different mapping approaches using NAM populations successfully exploited the genetics of complex traits and facilitated the discovery of candidate genes in rice (Fragoso et al. 2017), wheat (Hu et al. 2018; Jordan et al. 2018), maize (McMullen et al. 2009; Yu et al. 2008) and soybean (Song et al. 2017; Xavier et al. 2018). For NUE-related traits, significant genetic variations in hybrids, open-pollinated populations, large germplasm panels, backcross and recombinant inbred line populations in different cereal crops such as rice, wheat, maize and oilseed rape were observed (Chen et al. 2014; Vijayalakshmi et al. 2015; Li et al. 2015; He et al. 2017; Ertiro et al. 2017; Rao et al. 2018). Mapping for NUE related traits using different populations and mapping approaches highlight the complex nature of the trait.

In the present study, the nested synthetic wheat introgression libraries were designed for the identification of genomic regions associated with traits related to NUE using GWAS approach keeping into account the genetic effects produced in each genetic background. The associated SNPs were used to track the potential candidate genes associated with a particular trait of interest. The presence of high phenotypic variability in the nested synthetic introgression libraries coupled with the high marker density across the whole genome provided a strong base to the association mapping.

Interestingly, the genes responsive to nutrient uptake under water stress (Wang et al. 2017; Diédhiou et al. 2008; Janicka-Russak and Kabala 2015), shoot growth, root and plant development (Wang et al. 2017), nutrient uptake and transport of various nutrients (Wang et al. 2014; Weng et al. 2020; Takahashi et al. 2012) reported to be collocated with 126 Mb genomic region on chr 2D constituting 25 MTAs which stood out as hot-spot for different traits (FRW, DRW, FSW and DSW) in the present study. This indicates the positive interactions between root traits, nutrient uptake and plant growth and development. The 7.7 Mb region on short arm of Chr 6A constituting 17 SNPs associated with GY showed collocation with the genes that were directly or indirectly involved in improving grain yield in different cereal crops. These include the genes controlling flowering (Kania et al. 1997), panicle and seed development (Jain et al. 2007; Li et al. 2011), grain yield (Terao et al. 2010), resistance to pathogenesis (Taniguchi et al. 2013; Wang et al. 2014; Niño et al. 2020) and abiotic stress tolerance (Palusa et al. 2007; Brands and Ho, 2002). The MTAs associated with different root

traits such as RSA, RV, tips and forks in the present study were located near the earlier reported genes involved in regulating abscisic acid sensitivity and root growth development in Arabidopsis (Rodriguez et al. 2014) and adaptation under water stress conditions in wheat (Singh et al. 2017). Interestingly, the gene accelerating flowering in Arabidopsis (Hwang et al. 2019) was observed to be collocated with the SNP AX-95136655 associated with DTF on chr 3B in the present study. The colocation of identified MTAs with earlier reported genes controlling the photosynthetic traits, root development, plant growth, nutrient uptake and transport, flowering, resistance to pathogenesis and stress-responsive genes further confirms the contribution of these identified traits/MTAs in improving nitrogen uptake/utilization and grain yield under N limited conditions. The identified nitrogen insensitive breeding lines with favourable alleles in combination for the multiple traits might serve as potential donors for the development of nitrogen efficient wheat varieties.

Conclusions

The nested synthetic introgression libraries covering extensive phenotypic variability coupled with huge genome coverage was used to identify the significant MTAs associated with NUE related traits in wheat. Significant phenotypic variations for the NUE related traits, yield and yield related traits among genotypes, treatments, seasons and their interactions (genotype x treatment, genotype x season, treatment x season and genotype x treatment x season) were observed. Stable MTAs identified for different traits measured in the present study co-migrating with various genes associated with nitrogen uptake/utilization and improving grain yield may help to harness their benefits in genomics-assisted breeding programs. The identification of nitrogen efficient breeding lines may serve novel donors in genomics-assisted introgression programs. The identification and introgression of superior haplotype improving NUE while maintaining grain yield using haplotype-based breeding may open new avenues in designing next-generation nitrogen efficient high yielding wheat varieties.

Acknowledgments

We are thankful to the Department of Biotechnology, Govt. of India for providing grants.

Author contribution statement

NS and PC designed this study; AK provided the genotypic data of two populations and contributed to the development of nested introgression libraries; NS and MS conducted the

field experiments, NS analysed the data; NS, SK and PC provided resources; NS wrote the manuscript, and all co-authors revised the manuscript.

Funding

The work was compiled under projects funded by the Department of Biotechnology, Govt. of India (Grant No. BT/IN/UK-VNC/42/RG/2015-16 and BT/PR30871/BIC/101/1159/2018).

Data availability

The all-supported information's are available in supplementary material.

Declarations

Conflicts of interest

The authors declare that they no conflict of interests.

References

Allen AM, Winfield MO, Burridge AJ, Downie RC, Benbow HR, Barker GL, Wilkinson PA, Coghill J, Waterfall C, Davassi A, Scopes G (2017) Characterization of a Wheat Breeders' Array suitable for high-throughput SNP genotyping of global accessions of hexaploid bread wheat (*Triticum aestivum*). Plant Biotech J 15(3):390-401

An D, Su J, Liu Q, Zhu Y, Tong Y, Li J, Jing R, Li B, Li Z (2006) Mapping QTLs for nitrogen uptake in relation to the early growth of wheat (*Triticum aestivum L.*). Plant and Soil 284(1):73-84

Arcondéguy T, Jack R, Merrick M (2001) PII signal transduction proteins, pivotal players in microbial nitrogen control. Microbio Mol Bio Rev 65(1):80

Arnesano F, Banci L, Benvenuti M, Bertini I, Calderone V, Mangani S, Viezzoli MS (2003) The evolutionarily conserved trimeric structure of CutA1 proteins suggests a role in signal transduction. J Bio Chem 278(46):45999-6006

Bahrini I, Ogawa T, Kobayashi F, Kawahigashi H, Handa H (2011) Overexpression of the pathogen-inducible wheat TaWRKY45 gene confers disease resistance to multiple fungi in transgenic wheat plants. Breed Sci 61(4):319-236

Belete F, Dechassa N, Molla A, Tana T (2018) Effect of nitrogen fertilizer rates on grain yield and nitrogen uptake and use efficiency of bread wheat (*Triticum aestivum* L.) varieties on the Vertisols of central highlands of Ethiopia. Agri Food Sec 7(1):1-2

Bianchet C, Wong A, Quaglia M, Alqurashi M, Gehring C, Ntoukakis V, Pasqualini S (2019) An Arabidopsis thaliana leucine-rich repeat protein harbors an adenylyl cyclase catalytic center and affects responses to pathogens. J Plant Physio 232:12-22

Boeven PH, Longin CF, Leiser WL, Kollers S, Ebmeyer E, Würschum T (2016) Genetic architecture of male floral traits required for hybrid wheat breeding. Theor App Genet 129(12):2343-2357

Brands A, Ho TH. Function of a plant stress-induced gene, HVA22 (2002) Synthetic enhancement screen with its yeast homolog reveals its role in vesicular traffic. Plant Physio 130(3):1121-1131

Buchner P, Hawkesford MJ (2014) Complex phylogeny and gene expression patterns of members of the NITRATE TRANSPORTER 1/PEPTIDE TRANSPORTER family (NPF) in wheat. J Exp Bot 65(19):5697-5510

Burkhead JL, Abdel-Ghany SE, Morrill JM, Pilon-Smits EA, Pilon M (2003) The Arabidopsis thaliana CUTA gene encodes an evolutionarily conserved copper binding chloroplast protein. The Plant J 34(6):856-867

Cao A, Xing L, Wang X, Yang X, Wang W, Sun Y, Qian C, Ni J, Chen Y, Liu D, Wang X (2011) Serine/threonine kinase gene Stpk-V, a key member of powdery mildew resistance gene Pm21, confers powdery mildew resistance in wheat. Proc Nat Acad Sci 108(19):7727-32

Cavanagh CR, Chao S, Wang S, Huang BE, Stephen S, Kiani S, Forrest K, Saintenac C, Brown-Guedira GL, Akhunova A, See D (2013) Genome-wide comparative diversity uncovers multiple targets of selection for improvement in hexaploid wheat landraces and cultivars. Proc Nat Acad Sci 110(20):8057-8062

Chen B, Xu K, Li J, Li F, Qiao J, Li H, Gao G, Yan G, Wu X (2014) Evaluation of yield and agronomic traits and their genetic variation in 488 global collections of *Brassica napus* L. Genet Res Crop Evo 61(5):979-999

Chen L, Li YX, Li C, Shi Y, Song Y, Zhang D, Li Y, Wang T (2018) Genome-wide analysis of the pentatricopeptide repeat gene family in different maize genomes and its important role in kernel development. BMC Plant Bio 18(1):1-4

Chen L, Xiang S, Chen Y, Li D, Yu D (2017) Arabidopsis WRKY45 interacts with the DELLA protein RGL1 to positively regulate age-triggered leaf senescence. Mol Plant 10(9):1174-1189

Cheng Y, Qin G, Dai X, Zhao Y (2008) NPY genes and AGC kinases define two key steps in auxin-mediated organogenesis in Arabidopsis. Proc Nat Acad Sci 105(52):21017-21022

Cheng Z, Song F, Shan X, Wei Z, Wang Y, Dunaway-Mariano D, Gong W (2006) Crystal structure of human thioesterase superfamily member 2. Biochem Bio Res Com 349(1):172-177

Chevalier D, Batoux M, Fulton L, Pfister K, Yadav RK, Schellenberg M, Schneitz K (2005) STRUBBELIG defines a receptor kinase-mediated signaling pathway regulating organ development in Arabidopsis. Proc Nat Acad Sci 102(25):9074-9079

Choi HW, Lee BG, Kim NH, Park Y, Lim CW, Song HK, Hwang BK (2008) A role for a menthone reductase in resistance against microbial pathogens in plants. Plant Physio 148(1):383-401

Coque M, Martin A, Veyrieras JB, Hirel B, Gallais A (2008) Genetic variation for N-remobilization and postsilking N-uptake in a set of maize recombinant inbred lines: QTL detection and coincidences. Theor App Genet 117(5):729-747

Dai C, Xue HW (2010) Rice early flowering1, a CKI, phosphorylates DELLA protein SLR1 to negatively regulate gibberellin signalling. The EMBO J. 29(11):1916-1927

Deng Z, Cui Y, Han Q, Fang W, Li J, Tian J (2017) Discovery of consistent QTLs of wheat spike-related traits under nitrogen treatment at different development stages. Front Plant Sci 8:2120

Diédhiou CJ, Popova OV, Dietz KJ, Golldack D (2008) The SNF1-type serine-threonine protein kinase SAPK4 regulates stress-responsive gene expression in rice. BMC Plant Bio 8(1):1-3

Ding W, Lin L, Zhang B, Xiang X, Wu J, Pan Z, Zhu S (2015) OsKASI, a β-ketoacyl-[acyl carrier protein] synthase I, is involved in root development in rice (*Oryza sativa* L.). Planta 242(1):203-213

Earl DA (2012) STRUCTURE HARVESTER: a website and program for visualizing STRUCTURE output and implementing the Evanno method. Conser Genet Res 4(2):359-61

El-Esawi MA, Alayafi AA (2019) Overexpression of rice Rab7 gene improves drought and heat tolerance and increases grain yield in rice (*Oryza sativa* L.). Genes 10(1):56

Ertiro BT, Beyene Y, Das B, Mugo S, Olsen M, Oikeh S, Juma C, Labuschagne M, Prasanna BM (2017) Combining ability and testcross performance of drought-tolerant maize inbred lines under stress and non-stress environments in Kenya. Plant Breed 136(2):197-205

Fageria NK, De Morais OP, Dos Santos AB (2010). Nitrogen use efficiency in upland rice genotypes. J Plant Nut 33(11):1696-1711.

FAO (2019). FAO World Fertilizer Trends and Outlook to 2020. Available online at: http://www.fao.org/3/a-i6895e.pdf (accessed June 11, 2019).

Fontaine JX, Ravel C, Pageau K, Heumez E, Dubois F, Hirel B, Le Gouis J (2009) A quantitative genetic study for elucidating the contribution of glutamine synthetase, glutamate dehydrogenase and other nitrogen-related physiological traits to the agronomic performance of common wheat. Theor App Genet 119:645-662

Fujioka S (1997) The Arabidopsis deetiolated2 Mutant Is Blocked Early in Brassinosteroid Biosynthesis. The Plant Cell 9(11):1951-1962

Gaju O, Allard V, Martre P, Snape J, Heumez E, LeGouis J, Moreau D, Bogard M, Griffiths S, Orford S, Hubbart S, Foulkes M (2011) Identification of traits to improve the nitrogen-use efficiency of wheat genotypes. Field Crop Res 123:139-152

Gallego-Giraldo L, Posé S, Pattathil S, Peralta AG, Hahn MG, Ayre BG, Sunuwar J, Hernandez J, Patel M, Shah J, Rao X, (2018) Elicitors and defense gene induction in plants with altered lignin compositions. New Phytologist 219(4):1235-1251

Gangurde SS, Kumar R, Pandey AK, Burow M, Laza HE, Nayak SN, Guo B (2019) Climate-smart groundnuts for achieving high productivity and improved quality: current status, challenges, and opportunities. In Genomic Designing of Climate-Smart Oilseed Crops (Kole C, ed.), pp. 133-172. Cham: Springer Nature Switzerland AG.

Gerna D, Arc E, Holzknecht M, Roach T, Jansen-Dürr P, Weiss AK, Kranner I (2021) AtFAHD1a: A New Player Influencing Seed Longevity and Dormancy in Arabidopsis? Int J Mol Sci 22(6):2997

Gidda SK, Varin L (2006) Biochemical and molecular characterization of flavonoid 7-sulfotransferase from Arabidopsis thaliana. Plant Physio Biochem 44(11-12):628-636

Habash DZ, Bernard S, Schondelmaier J, Weyen J, Quarrie SA (2007) The genetics of nitrogen use in hexaploid wheat: N utilisation, development and yield. Theor App Genet 14(3):403-419

Hawkesford MJ, Griffiths S (2019) Exploiting genetic variation in nitrogen use efficiency for cereal crop improvement. Current Opin Plant Bio 49:35-42

He H, Yang R, Li Y, Ma A, Cao L, Wu X, Chen B, Tian H, Gao Y (2017) Genotypic variation in nitrogen utilization efficiency of oilseed rape (Brassica napus) under contrasting N supply in pot and field experiments. Front Plant Sci 8:1825

Hickman JE, Palm CA, Mutuo P, Melillo JM, Tang J (2014) Nitrous oxide (N_2O) emissions in response to increasing fertilizer addition in maize (*Zea mays* L.) agriculture in western Kenya. Nut Cycl Agroecosys 100(2):177-187

Hori K, Ogiso-Tanaka E, Matsubara K, Yamanouchi U, Ebana K, Yano M (2013) H d16, a gene for casein kinase I, is involved in the control of rice flowering time by modulating the day-length response. The Plant J 76(1):36-46.

Hu J, Guo C, Wang B, Ye J, Liu M, Wu Z, Xiao Y, Zhang Q, Li H, King GJ, Liu K (2018) Genetic properties of a nested association mapping population constructed with semi-winter and spring oilseed rapes. Front Plant Sci 9:1740

Hwang K, Susila H, Nasim Z, Jung JY, Ahn JH (2019) Arabidopsis ABF3 and ABF4 transcription factors act with the NF-YC complex to regulate SOC1 expression and mediate drought-accelerated flowering. Mol Plant 12(4):489-505

Jain M, Nijhawan A, Arora R, Agarwal P, Ray S, Sharma P, Kapoor S, Tyagi AK, Khurana JP (2007) F-box proteins in rice. Genome-wide analysis, classification, temporal and spatial gene expression during panicle and seed development, and regulation by light and abiotic stress. Plant Physio 143(4):1467-1483

Janiak A, Kwaśniewski M, Szarejko I (2016) Gene expression regulation in roots under drought. J Exp Bot 67(4):1003-1014

Janicka-Russak M, Kabała K (2015) The role of plasma membrane H+-ATPase in salinity stress of plants. InProgress in Botany 2015 (pp. 77-92). Springer, Cham

Jordan KW, Wang S, He F, Chao S, Lun Y, Paux E, Sourdille P, Sherman J, Akhunova A, Blake NK, Pumphrey MO (2018) The genetic architecture of genome-wide recombination rate variation in allopolyploid wheat revealed by nested association mapping. The Plant J 95(6):1039-1054

Jung YJ, Melencion SM, Lee ES, Park JH, Alinapon CV, Oh HT, Yun DJ, Chi YH, Lee SY (2015) Universal stress protein exhibits a redox-dependent chaperone function in Arabidopsis and enhances plant tolerance to heat shock and oxidative stress. Front Plant Sci 6:1141

Kang J, Park J, Choi H, Burla B, Kretzschmar T, Lee Y, Martinoia E (2011) Plant ABC transporters. The Arabidopsis book/American Society of Plant Biologists 9

Kania T, Russenberger D, Peng S, Apel K, Melzer S. FPF1 promotes flowering in Arabidopsis. The Plant Cell. 1997 Aug 1;9(8):1327-1338

Kim H, Lee SB, Kim HJ, Min MK, Hwang I, Suh MC (2012) Characterization of glycosylphosphatidylinositol-anchored lipid transfer protein 2 (LTPG2) and overlapping function between LTPG/LTPG1 and LTPG2 in cuticular wax export or accumulation in Arabidopsis thaliana. Plant Cell Physio 53(8):1391-1403

Kim MJ, Go YS, Lee SB, Kim YS, Shin JS, Min MK, Hwang I, Suh MC (2010) Seed-expressed casein kinase I acts as a positive regulator of the SeFAD2 promoter via phosphorylation of the SebHLH transcription factor. Plant Mol Bio 73(4-5):425-437

Kitagawa K, Kurinami S, Oki K, Abe Y, Ando T, Kono I, Yano M, Kitano H, Iwasaki Y (2010) A novel kinesin 13 protein regulating rice seed length. Plant Cell Physio 51(8):1315-1329.

Kobayashi Y, Motose H, Iwamoto K, Fukuda H (2011) Expression and genome-wide analysis of the xylogen-type gene family. Plant Cell Physio 52(6):1095-1106

Laperche A, Le Gouis J, Hanocq E, Brancourt-Hulmel M (2008) Modelling nitrogen stress with probe genotypes to assess genetic parameters and genetic determinism of winter wheat tolerance to nitrogen constraint. Euphytica 161(1):259-271

Lee K, Park SJ, Han JH, Jeon Y, Pai HS, Kang H (2019) A chloroplast-targeted pentatricopeptide repeat protein PPR287 is crucial for chloroplast function and Arabidopsis development. BMC Plant Bio 19(1):1-10

Lesniewicz K, Karlowski WM, Pienkowska JR, Krzywkowski P, Poreba E (2013) The plant S1-like nuclease family has evolved a highly diverse range of catalytic capabilities. Plant and Cell Physio 54(7):1064-1078

Leterrier M, Chaki M, Airaki M, Valderrama R, Palma JM, Barroso JB, Corpas FJ. Function of S-nitrosoglutathione reductase (GSNOR) in plant development and under biotic/abiotic stress. Plant Signaling & Behavior. 2011 Jun 1;6(6):789-93.

Li M, Tang D, Wang K, Wu X, Lu L, Yu H, Gu M, Yan C, Cheng Z (2011) Mutations in the F-box gene LARGER PANICLE improve the panicle architecture and enhance the grain yield in rice. Plant Biotech J (9):1002-1013

Li P, Chen F, Cai H, Liu J, Pan Q, Liu Z, Gu R, Mi G, Zhang F, Yuan L (2015) A genetic relationship between nitrogen use efficiency and seedling root traits in maize as revealed by QTL analysis. J Exp Bot 66(11):3175-3188
Li Y, Dai X, Cheng Y, Zhao Y (2011) NPY genes play an essential role in root gravitropic responses in Arabidopsis. Mol Plant 4(1):171-179
Li YD, Wang YJ, Tong YP, Gao JG, Zhang JS, Chen SY (2005). QTL mapping of phosphorus deficiency tolerance in soybean (Glycine max L. Merr.). Euphytica 142(1):137-142.
Liang Q, Cheng X, Mei M, Yan X, Liao H (2010) QTL analysis of root traits as related to phosphorus efficiency in soybean. Ann Bot 106(1):223-234
Liao H, Yan X, Rubio G, Beebe SE, Blair MW, Lynch JP (2004) Genetic mapping of basal root gravitropism and phosphorus acquisition efficiency in common bean. Funct Plant Bio 31(10):959-970
Lin ZJ, Liebrand TW, Yadeta KA, Coaker G (2015) PBL13 is a serine/threonine protein kinase that negatively regulates Arabidopsis immune responses. Plant Physio 169(4):2950-62.
Liu F, Zhang X, Lu C, Zeng X, Li Y, Fu D, Wu G (2015) Non-specific lipid transfer proteins in plants: presenting new advances and an integrated functional analysis. J Exp Bot 66(19):5663-5681
Liu H, Hu M, Wang Q, Cheng L, Zhang Z (2018) Role of papain-like cysteine proteases in plant development. Front Plant Sci 9:1717
Liu WX, Zhang FC, Zhang WZ, Song LF, Wu WH, Chen YF (2013) Arabidopsis Di19 functions as a transcription factor and modulates PR1, PR2, and PR5 expression in response to drought stress. Mol Plant 6(5):1487-1502
Mackay IJ, Bansept-Basler P, Barber T, Bentley AR, Cockram J, Gosman N, Greenland AJ, Horsnell R, Howells R, O'Sullivan DM, Rose GA (2014) An eight-parent multiparent advanced generation inter-cross population for winter-sown wheat: creation, properties, and validation. G3: Genes Genom Genet 4(9):1603-1610
Mahjourimajd S, Kuchel H, Langridge P, Okamoto M (2016) Evaluation of Australian wheat genotypes for response to variable nitrogen application. Plant and Soil 399(1-2):247-255
McGinnis KM (2003) The Arabidopsis SLEEPY1 Gene Encodes a Putative F-Box Subunit of an SCF E3 Ubiquitin Ligase. The Plant Cell 15(5):1120-1130
McMullen MD, Kresovich S, Villeda HS, Bradbury P, Li H, Sun Q, Flint-Garcia S, Thornsberry J, Acharya C, Bottoms C, Brown P (2009) Genetic properties of the maize nested association mapping population. Science 325(5941):737-740
Ming F, Zheng X, Mi G, He P, Zhu L, Zhang F (2000) Identification of quantitative trait loci affecting tolerance to low phosphorus in rice (*Oryza Sativa* L.). Chinese Sci Bull 45(6):520-525
Mo P, Zhu Y, Liu X, Zhang A, Yan C, Wang D (2007) Identification of two phosphatidylinositol/phosphatidylcholine transfer protein genes that are predominately transcribed in the flowers of Arabidopsis thaliana. J Plant Physio 164(4):478-486
Mok DW, Mok MC (2001) Cytokinin metabolism and action. Ann Rev Plant Bio 52(1):89-118
Morita S, Suga T, Yamazaki K (1988) The relationship between root length density and yield in rice plants. Jpn J Crop Sci 57:438-443
Motose H, Sugiyama M, Fukuda H, (2004) A proteoglycan mediates inductive interaction during plant vascular development. Nature 429(6994):873-878
Naveed Afzal Z, Huguet-Tapia JC, Ali GS (2019) Transcriptome profile of Carrizo citrange roots in response to Phytophthora parasitica infection. J Plant Inter 14(1):187-204
Ni W, Xu SL, González-Grandío E, Chalkley RJ, Huhmer AF, Burlingame AL, Wang ZY, Quail PH (2017) PPKs mediate direct signal transfer from phytochrome photoreceptors to transcription factor PIF3. Nature Comm 8(1):1-1
Ninfa AJ, Atkinson MR (2000) PII signal transduction proteins. Trends Micro 8(4):172-179

Niño MC, Kang KK, Cho YG (2020) Genome-wide transcriptional response of papain-like cysteine protease-mediated resistance against *Xanthomonas oryzae* pv. *oryzae* in rice. Plant Cell Rep 39(4):457-472.

Obara M, Sato T, Sasaki S, Kashiba K, Nagano A, Nakamura I, Ebitani T, Yano M, Yamaya T (2004) Identification and characterization of a QTL on chromosome 2 for cytosolic glutamine synthetase content and panicle number in rice. Theor App Genet 110(1):1-1

Orsel M, Chopin F, Leleu O, Smith SJ, Krapp A, Daniel-Vedele F, Miller AJ (2006) Characterization of a two-component high-affinity nitrate uptake system in Arabidopsis. Physiology and protein-protein interaction. Plant Physio 142(3):1304-1317

Palusa SG, Ali GS, Reddy AS (2007) Alternative splicing of pre-mRNAs of Arabidopsis serine/arginine-rich proteins: regulation by hormones and stresses. The Plant J 49(6):1091-1107

Pandey MK, Monyo E, Ozias-Akins P, Liang X, Guimarães P, Nigam SN, Upadhyaya HD, Janila P, Zhang X, Guo B, Cook DR (2012) Advances in Arachis genomics for peanut improvement. Biotech Adv 30(3):639-651

Pandey MK, Roorkiwal M, Singh VK, Ramalingam A, Kudapa H, Thudi M, Chitikineni A, Rathore A, Varshney RK (2016) Emerging genomic tools for legume breeding: current status and future prospects. Front Plant Sci 7:455

Poon WW, Davis DE, Ha HT, Jonassen T, Rather PN, Clarke CF (2000) Identification of Escherichia coli ubiB, a gene required for the first monooxygenase step in ubiquinone biosynthesis. J Bacteria 82(18):5139

Prasad M, Varshney RK, Kumar A, Balyan HS, Sharma PC, Edwards KJ, Dhaliwal HS, Roy JK, Gupta PK (1999) A microsatellite marker associated with a QTL for grain protein content on chromosome arm 2DL of bread wheat. Theor App Genet 99(1):341-345

Pritchard JK, Wen W (2004) Documentation for the STRUCTURE software Version 2. Chicago.

Purcell S, Neale B, Todd-Brown K, Thomas L, Ferreira MA, Bender D, Maller J, Sklar P, De Bakker PI, Daly MJ, Sham PC (2007) PLINK: a tool set for whole-genome association and population-based linkage analyses. The Amer J Hum Genet 81(3):559-575

Qian Y, Chen C, Jiang L, Zhang J, Ren Q (2019) Genome-wide identification, classification and expression analysis of the JmjC domain-containing histone demethylase gene family in maize. BMC Genom 20(1):256

Quesada V (2016) The roles of mitochondrial transcription termination factors (MTERFs) in plants. Physio Plant 157(3):389-399

Rao IS, Neeraja CN, Srikanth B, Subrahmanyam D, Swamy KN, Rajesh K, Vijayalakshmi P, Kiran TV, Sailaja N, Revathi P, Rao PR (2018) Identification of rice landraces with promising yield and the associated genomic regions under low nitrogen. Sci Rep 8(1):1-3

Rasheed A, Xia X (2019) From markers to genome-based breeding in wheat. Theor App Genet 132(3):767-784

Rautengarten C, Usadel B, Neumetzler L, Hartmann J, Büssis D, Altmann T (2008) A subtilisin-like serine protease essential for mucilage release from Arabidopsis seed coats. The Plant J 54(3):466-480

Reddy PP (2017) Fertilizer Management. In: Agro-ecological Approaches to Pest Management for Sustainable Agriculture. Springer, Singapore. https://doi.org/10.1007/978-981-10-4325-3_5

Rivas S, Rougon-Cardoso A, Smoker M, Schauser L, Yoshioka H, Jones JD (2004) Retraction: CITRX thioredoxin interacts with the tomato Cf-9 resistance protein and negatively regulates defence. The EMBO J 23(10):2156-2165

Rober-Kleber N, Albrechtová JT, Fleig S, Huck N, Michalke W, Wagner E, Speth V, Neuhaus G, Fischer-Iglesias C (2003) Plasma membrane H^+-ATPase is involved in auxin-mediated cell elongation during wheat embryo development. Plant Physio 131(3):1302-1312

Rodriguez L, Gonzalez-Guzman M, Diaz M, Rodrigues A, Izquierdo-Garcia AC, Peirats-Llobet M, Fernandez MA, Antoni R, Fernandez D, Marquez JA, Mulet JM (2014) C2-domain abscisic acid-related proteins mediate the interaction of PYR/PYL/RCAR abscisic acid receptors with the plasma membrane and regulate abscisic acid sensitivity in Arabidopsis. The Plant Cell 26(12):4802-4820

Russo TA, Tully K, Palm C, Neill C (2017) Leaching losses from Kenyan maize cropland receiving different rates of nitrogen fertilizer. Nut Cyc Agro 108(2):195-209

Sandhu N, Subedi SR, Singh VK, Sinha P, Kumar S, Singh SP, Ghimire SK, Pandey M, Yadaw RB, Varshney RK, Kumar A (2019) Deciphering the genetic basis of root morphology, nutrient uptake, yield, and yield-related traits in rice under dry direct- seeded cultivation systems. Sci Rep 9(1):9334

Sandhu N, Torres RO, Sta Cruz MT, Maturan PC, Jain R, Kumar A, Henry A (2015) Traits and QTLs for development of dry direct-seeded rainfed rice varieties. J Exp Bot 66(1):225-244

Šarčević H, Jukić K, Ikić I, Lovrić A (2014) Estimation of quantitative genetic parameters for grain yield and quality in winter wheat under high and low nitrogen fertilization. Euphytica 199(1):57-67

Scott MF, Ladejobi O, Amer S, Bentley AR, Biernaskie J, Boden SA, Clark M, Dell'Acqua M, Dixon LE, Filippi CV, Fradgley N (2020) Multi-parent populations in crops: A toolbox integrating genomics and genetic mapping with breeding. Heredity 125(6):396-416

Shimono M, Sugano S, Nakayama A, Jiang CJ, Ono K, Toki S, Takatsuji H (2007) Rice WRKY45 plays a crucial role in benzothiadiazole-inducible blast resistance. The Plant Cell 19(6):2064-2076

Sial MA, Arain MA, Khanzada SH, Naqvi MH, Dahot MU, Nizamani NA (2005) Yield and quality parameters of wheat genotypes as affected by sowing dates and high temperature stress. Pak J Bot 37(3):575

Steinfeld B, Scott J, Vilander G, Marx L, Quirk M, Lindberg J, Koerner K (2015) The role of lean process improvement in implementation of evidence-based practices in behavioural health care. The J Bev Health Ser Res 42(4):504-518

Skylar A, Sung F, Hong F, Chory J, Wu X (2011) Metabolic sugar signal promotes Arabidopsis meristematic proliferation via G2. Dev Bio 351(1):82-89

Srikanth B, Rao IS, Surekha K, Subrahmanyam D, Voleti SR, Neeraja CN (2016) Enhanced expression of OsSPL14 gene and its association with yield components in rice (*Oryza sativa*) under low nitrogen conditions. Gene 576(1):441-450

Steffens B, Rasmussen A (2016) The physiology of adventitious roots. Plant Physio 170:603-617

Su J, Xiao Y, Li M, Liu Q, Li B, Tong Y, Jia J, Li Z (2006) Mapping QTLs for phosphorus-deficiency tolerance at wheat seedling stage. Plant and Soil 281(1):25-36

Su JY, Zheng Q, Li HW, Li B, Jing RL, Tong YP, Li ZS (2009) Detection of QTLs for phosphorus use efficiency in relation to agronomic performance of wheat grown under phosphorus sufficient and limited conditions. Plant Sci 176(6):824-836

Subedi SR, Sandhu N, Singh VK, Sinha P, Kumar S, Singh SP, Gimire SK, Pandey M, Yadaw RB, Varshney RK, Kumar A (2019) Genome-wide association study reveals significant genomic regions for improving yield, adaptability of rice under dry direct seeded cultivation condition. BMC Genom 20(1):471

Sun H, Qian Q, Wu K, Luo J, Wang S, Zhang C, Ma Y, Liu Q, Huang X, Yuan Q, Han R (2014) Heterotrimeric G proteins regulate nitrogen-use efficiency in rice. Nat Genet 46(6):652-656

Takahashi K, Hayashi KI, Kinoshita T (2012) Auxin activates the plasma membrane H^+-ATPase by phosphorylation during hypocotyl elongation in Arabidopsis. Plant Physio 159(2):632-641

Taniguchi S, Hosokawa-Shinonaga Y, Tamaoki D, Yamada S, Akimitsu K, Gomi K (2014) Jasmonate induction of the monoterpene linalool confers resistance to rice bacterial blight and its biosynthesis is regulated by JAZ protein in rice. Plant, Cell Environ 37(2):451-461

Terao T, Nagata K, Morino K, Hirose T (2010) A gene controlling the number of primary rachis branches also controls the vascular bundle formation and hence is responsible to increase the harvest index and grain yield in rice. Theor App Genet 120(5):875-893

Varshney RK, Mohan SM, Gaur PM, Gangarao NVPR, Pandey MK, Bohra A, Sawargaonkar SL (2013) Achievements and prospects of genomics-assisted breeding in three legume crops of the semi-arid tropics. Biotechnol Adv 31:1120-1134

Vijayalakshmi P, Vishnukiran T, Kumari BR, Srikanth B, Rao IS, Swamy KN 2015 Biochemical and physiological characterization for nitrogen use efficiency in aromatic rice genotypes. Field Crops Res 179:132-143

Wang H, Xu Q, Kong YH, Chen Y, Duan JY, Wu WH, Chen YF (2014) Arabidopsis WRKY45 transcription factor activates PHOSPHATE TRANSPORTER1; 1 expression in response to phosphate starvation. Plant Physio 164(4):2020-2029

Wang S, Wong D, Forrest K, Allen A, Chao S, Huang BE, Maccaferri M, Salvi S, Milner SG, Cattivelli L, Mastrangelo AM (2014) Characterization of polyploid wheat genomic diversity using a high-density 90 000 single nucleotide polymorphism array. Plant Biotech J 12(6):787-796.

Wang Y, Cordewener JH, America AH, Shan W, Bouwmeester K, Govers F (2015) Arabidopsis lectin receptor kinases LecRK-IX. 1 and LecRK-IX. 2 are functional analogs in regulating Phytophthora resistance and plant cell death. Mol Plant-Microbe Inter 28(9):1032-1048

Wang Y, Pang C, Li X, Hu Z, Lv Z, Zheng B, Chen, P (2017) Identification of tRNA nucleoside modification genes critical for stress response and development in rice and Arabidopsis. BMC Plant Bio 17(1)1-15

Weinitschke S, Denger K, Cook AM, Smits TH (2007) The DUF81 protein TauE in Cupriavidus necator H16, a sulfite exporter in the metabolism of C2 sulfonates. Microbiology 153(9):3055-3060

Weng L, Zhang M, Wang K, Chen G, Ding M, Yuan W, Zhu Y, Xu W, Xu F (2020) Potassium alleviates ammonium toxicity in rice by reducing its uptake through activation of plasma membrane H^+-ATPase to enhance proton extrusion. Plant Physio Biochem 151:429-437

Winfield MO, Allen AM, Burridge AJ, Barker GL, Benbow HR, Wilkinson PA, Coghill J, Waterfall C, Davassi A, Scopes G, Pirani A (2016) High-density SNP genotyping array for hexaploid wheat and its secondary and tertiary gene pool. Plant Biotech J 14(5):1195-1206

Winkel-Shirley B (2001) Flavonoid biosynthesis. A colorful model for genetics, biochemistry, cell biology, and biotechnology. Plant Physio 126(2):485-493

Wissuwa M, Yano M, Ae N (1998) Mapping of QTLs for phosphorus-deficiency tolerance in rice (Oryza sativa L.). Theor App Genet 97(5-6):777-783

Wollmann H, Stroud H, Yelagandula R, Tarutani Y, Jiang D, Jing L, Jamge B, Takeuchi H, Holec S, Nie X, Kakutani T (2017) The histone H3 variant H3. 3 regulates gene body DNA methylation in Arabidopsis thaliana. Genome Bio 18(1):1-10

Xavier A, Xu S, Muir WM, Rainey KM (2015) NAM: association studies in multiple populations. Bioinformatics 31(23):3862-3864

Xiong H, Li J, Liu P, Duan J, Zhao Y, Guo X, Li Y, Zhang H, Ali J, Li Z (2014) Overexpression of OsMYB48-1, a novel MYB-related transcription factor, enhances drought and salinity tolerance in rice. PloS One 9(3):e92913

Xu Y, Wang R, Tong Y, Zhao H, Xie Q, Liu D, Zhang A, Li B, Xu H, An D (2014) Mapping QTLs for yield and nitrogen-related traits in wheat: influence of nitrogen and phosphorus fertilization on QTL expression. Theor App Genet 127(1):59-72

Yamaya T, Obara M, Nakajima H, Sasaki S, Hayakawa T, Sato T (2002) Genetic manipulation and quantitative-trait loci mapping for nitrogen recycling in rice. J Exp Bot 53(370):917-25

Yan X, Liao H, Beebe SE, Blair MW, Lynch JP (2004) QTL mapping of root hair and acid exudation traits and their relationship to phosphorus uptake in common bean. Plant Soil 265, 17-29.

Yang JC, Zhang H, Zhang JH (2012) Root morphology and physiology in relation to the yield formation of rice. J Integr Agric 11:920-926

Yang L, Ji W, Zhu Y, Gao P, Li Y, Cai H, Bai X, Guo D (2010) GsCBRLK, a calcium/calmodulin-binding receptor-like kinase, is a positive regulator of plant tolerance to salt and ABA stress. J Exp Bot 61(9):2519-2533

Yao L, Cheng X, Gu Z, Huang W, Li S, Wang L, Wang YF, Xu P, Ma H, Ge X (2018) The AWPM-19 family protein OsPM1 mediates abscisic acid influx and drought response in rice. The Plant Cell 30(6):1258-1276

Yokoo T, Saito H, Yoshitake Y, Xu Q, Asami T, Tsukiyama T, Teraishi M, Okumoto Y, Tanisaka T (2014) Se14, encoding a JmjC domain-containing protein, plays key roles in long-day suppression of rice flowering through the demethylation of H3K4me3 of RFT1. PLoS One 9(4):e96064

Yu J, Holland JB, McMullen, MD Buckler ES (2008) Genetic design and statistical power of nested association mapping in maize. Genetics 178:539-551

Yu W, Kan Q, Zhang J, Chen Q (2015) Role of the plasma membrane [H^+-ATPase in the regulation of organic acid exudation under aluminium toxicity and phosphorus deficiency. Plant Signal Behav 1:e1106660

Yuan H, Liu D (2012) Functional disruption of the pentatricopeptide protein SLG1 affects mitochondrial RNA editing, plant development, and responses to abiotic stresses in Arabidopsis. Plant J. 70:432-444

Yun HS, Kwaaitaal M, Kato N, Yi C, Park S, Sato MH, Schulze-Lefert P, Kwon C (2013) Requirement of vesicle-associated membrane protein 721 and 722 for sustained growth during immune responses in Arabidopsis. Molecules and Cells 35(6):481-488

Zhang M, Chen C, Froehlich JE, TerBush AD, Osteryoung KW (2015) Roles of Arabidopsis PARC6 in Coordination of the Chloroplast Division Complex and Negative Regulation of FtsZ Assembly. Plant Physiology, 170(1):250-262

Zhao K, Tung CW, Eizenga GC, Wright MH, Ali ML, Price AH, Norton GJ, Islam MR, Reynolds A, Mezey J, McClung AM, Bustamante CD, SR MC (2011) Genome-wide association mapping reveals a rich genetic architecture of complex traits in *Oryza sativa*. Nat Commun 2:467

Zhao YF, Peng T, Sun HZ, Teotia S, Wen HL, Du YX, Zhang J, Li JZ, Tang GL, Xue HW, Zhao QZ (2019) miR1432-Os ACOT (Acyl-CoA thioesterase) module determines grain yield via enhancing grain filling rate in rice. Plant Biotech J 17(4):712-723

Zheng N, Fraenkel E, Pabo CO, Pavletich NP (1999) Structural basis of DNA recognition by the heterodimeric cell cycle transcription factor E2F-DP. Genes Develop 13(6):666-674

Zhou S, Wang Y, Li W, Zhao Z, Ren Y, Wang Y, Gu S, Lin Q, Wang D, Jiang L, Su N (2011) Pollen semi-sterility1 encodes a kinesin-1–like protein important for male meiosis, anther dehiscence, and fertility in rice. The Plant Cell 23(1):111-129

Zhu Y, Li T, Xu J, Wang J, Wang L, Zou W, Zeng D, Zhu L, Chen G, Hu J, Gao Z (2020) Leaf width gene LW5/D1 affects plant architecture and yield in rice by regulating nitrogen utilization efficiency. Plant Physio Biochem 157:359-369

Zhu J, Kaeppler SM, Lynch JP (2005) Mapping of QTL controlling root hair length in maize (*Zea mays* L.) under phosphorus deficiency. Plant Soil 270:299-310

Zhu XX, Li QY, Shen CC, Duan ZB, Yu DY, Niu JS, Ni YJ, Jiang YM (2016) Transcriptome analysis for abnormal spike development of the wheat mutant dms. PloS One 11(3):p.e0149287

Table 1 Details on experiments conducted in 2018-2019 and 2019-2020 rabi season

Pop	Pedigree	Total no lines	Design
Pop1	PDW233-*Ae. tauschii* acc. pau14135 amphiploid // BWL4444	75	Augmented/ Split plot design, nitrogen level main plot, breeding lines as Subplots, 2 replications, 2 rows plot (1.5 m long with 20 cm row to row spacing)
Pop2	PDW233-*Ae. tauschii* acc. pau 14135 amphiploid // BWL3531	106	Augmented design/ Split plot design, nitrogen level main plot, breeding lines as Subplots, 2 replications, 2 rows plot (1.5 m long with 20 cm row to row spacing)
Pop3	PBW114-*Ae. tauschii* acc. pau 14170 amphiploid//BWL4444	88	Split plot design, nitrogen level main plot, breeding lines as Subplots, 2 replications, 1.5 m x 2 rows plot
Pop4	PBW114-*Ae. tauschii* acc. pau 14170 amphiploid//BWL3531	83	Split plot design, nitrogen level main plot, breeding lines as Subplots, 2 replications, 1.5 m x 2 rows plot

Table 2 Analysis of variance (ANOVA) for the NUE related, root, plant morphological, yield and yield related traits among G (genotypes), (T) treatments, (S) seasons and their interactions (G x T, genotype x treatment; G x S, genotype x season; T x S, treatment x season; and G x T x S, genotype x treatment x season)

Population		LCC	SPAD	FRW	DRW	FSW	DSW	DTF	NPT	PHT	SPS	SB	FLL	FLW	GY	TRL	RSA	AD	RV	Tips	Forks
PDW233/ *Ae. tauschii*	G	7.45 ***	4.47 ***	2.44 ***	1.89 ***	5.84 ***	7.2 ***	58.79 ***	3.22 ***	4.9 **	4.92 *	2.27 ***	35.01 ***	88.48 ***	5.14 ***	1.56 **	3.90 *	0.872	3..81 *	8.84 ***	3.13 ***
14135 amphiploid/ / BWL4444	T	244.8 ***	286.5 ***	27.12 ***	56.14 ***	88.41 ***	55.36 ***	141.44 ***	254.3 ***	4.26 *	5.29 **	56.37 ***	120.87 ***	261.42 ***	14.18 ***	73.78 ***	27.41 ***	48.15 ***	6.5 **	125.1 *	86.92 ***
	S	612.8 ***	637.2 ***	117.9 ***	18.49 ***	447.45 ***	394.06 ***	6054.2 ***	30.88 ***	4.04 *	2.08*	7.22 **	24196 ***	44138 ***	109.4 ***	124.8 ***	4.93 *	90.05 ***	1.269 *	1062 ***	277.8 ***
	G x T	4.60 ***	2.19 ***	1.78 ***	1.62 ***	2.07 ***	2.76 ***	2.07 ***	3.49 ***	5.81 **	3.88*	2.04 ***	1.65 ***	34.33 ***	1.49 **	1.31 *	2.99 *	0.672	1 .87 *	3.70 ***	1.71 ***
	G x S	7.38 ***	3.2 ***	3.61 ***	1.8 ***	3.28 ***	3.79 ***	10.34 ***	1.84 ***	5.04 *	3.07*	1.74 **	1.84 ***	53.87 ***	1.798 ***	1.32 *	2.72 *	0.205	1.41 *	9.90 ***	3.37 ***
	T x S	3.24 *	10.53 ***	8.45 ***	8.22 ***	130.87 ***	56.21 ***	68.42 ***	44.65 ***	6.07 **	2.81*	116.6 ***	42.47 ***	572.6 ***	20.84 ***	3.69 *	4.45 **	21.75 ***	3.212 *	22.46 ***	11.50 ***
	G x T x S	6.62 ***	2.06 ***	1.855 ***	1.12	2.78 ***	3.21 ***	2.98 ***	1.94 ***	6.45 **	4.44 **	1.88 ***	5.92 *	67.56 ***	1.53 **	1.19 *	2.64 *	0.397	1.47 *	5.95 ***	1.87 ***
PDW233/ *Ae. tauschii*	G	6.83 *	4.8*	1.45 **	4.58 ***	2.45 ***	2.87 ***	60.11 ***	2.76 ***	3.65 ***	7.15 ***	2.20 ***	15.97 ***	106.4 ***	4.93 ***	3.73 ***	1.38 *	4.15 ***	2.76 *	5.02 ***	3.94 ***
14135 amphiploid/ / BWL3531	T	1.899 *	3.5*	2.94 **	5.10 **	53.34 ***	41.31 ***	188.7 ***	401 ***	135.5 ***	3.75 **	74.41 ***	83.24 ***	420.3 ***	62.89 ***	44.36 ***	9.05 ***	65.06 ***	2.13 *	82.64 ***	53.1 ***
	S	5.14 *	5.5*	25.45 ***	81.57 ***	420.24 ***	1089.9 ***	14660 ***	1.76 *	139.8 ***	26.57 ***	3.12 **	13821 ***	89346 ***	62.44 ***	1809 ***	334 ***	242.5 ***	2.03 *	2244 ***	1871 ***
	G x T	4.82 *	4.8*	1.52 ***	4.98 *	1.26 *	1.49 ***	2.33 ***	2.35 ***	2.31 ***	3.26 *	1.63 ***	1.27 *	2.96 ***	1.71 ***	1.41 *	2.99 *	3.54 *	2.82 *	2.05 ***	1.40 **
	G x S	4.36 *	3.3*	1.71 ***	3.73 *	1.37 *	1.29 *	9.23 ***	1.91 ***	2.73 ***	3.11 *	2.93 **	1.34 *	5.07 ***	1.84 ***	1.62 ***	2.61 *	2.42 *	3.31 *	2.86 ***	2.04 ***
	T x S	3.06 *	3.1*	17.76 ***	9.11 ***	36.98 ***	9.09 ***	126.58 ***	97.34 ***	2.74 *	3.19 *	193.4 ***	34.09 ***	976.9 ***	39.24 ***	279.4 ***	85.6 ***	39.58 ***	3.57 *	268.6 ***	247 ***
	G x T x S	4.41 *	4.4*	1.43 **	4.70 *	1.50 ***	1.43 *	2.69 ***	1.25 *	2.02 ***	2.99 *	1.39 **	1.68 *	2.86 ***	1.79 ***	1.37 **	3.62 *	3.27*	2.41 *	3.27 ***	1.93 ***
PBW114/ *Ae. tauschii*	G	2.24 ***	2.3 ***	1.94 ***	3.15 *	1.42 *	1.63 **	3.40 ***	1.60 **	3.22 ***	1.45 **	1.54 **	1.65 ***	1.49 ***	1.81 ***	2.01 ***	1.31 *	11.06 ***	2.78 *	2.15 *	1.66 ***
14170 amphiploid/ / BWL3531	T	259.26 ***	297.6 ***	51.44 ***	14.33 ***	9.25 ***	4.96 *	58.11 ***	267.6 ***	231.5 ***	19.11 ***	224.3 ***	398.9 ***	220.0 ***	61.77 ***	17.10 ***	30.7 ***	120.7 ***	33.84 ***	13.21 ***	14.9 ***
	S	42.69 ***	2.94 *	565.7 ***	2.69 *	11.69 ***	248.86 ***	8439.4 ***	1.24 *	98.01 ***	893 ***	59.26 ***	1026 ***	1364 ***	2.10*	1122 ***	516 ***	653.7 ***	4.69 *	449 **	682 ***

	G x T	2.65***	2.58***	2.22***	1.35**	1.43**	1.47**	3.78***	1.67***	2.80***	1.75*	1.34*	1.26*	1.68***	1.74***	2.46***	1.37**	2.94*	2.94*	1.42**	1.79***
	G x S	2.55***	3.01***	2.0***	1.50**	1.78*	1.43*	2.70***	2.03***	3.99***	1.74*	1.54*	1.79***	2.04***	1.49*	1.80***	0.97	2.94*	3.67*	1.99*	1.58**
	T x S	90.59***	95.61***	51.14***	13.09***	78.71***	18.81***	13.57***	163.8***	21.45***	10.34***	69.76***	21.72***	584***	17.82***	43.22***	4.05*	120.5***	25.83***	31.73***	20.1***
	G x T x S	2.10***	2.14***	1.89***	1.25*	1.53***	1.80*	3.75***	1.58***	3.32***	1.26*	1.26*	1.41**	1.65***	1.71***	2.43***	1.36**	2.94*	2.90*	1.46**	1.79***
PBW114/ *Ae. tauschii*	G	2.05*	3.0**	1.54*	2.99*	2.13*	1.94*	1.47**	1.29*	1.99*	1.32*	1.68***	1.54*	1.64***	1.87*	1.48**	1.98*	1.15	1.99*	1.54**	1.56**
14170 amphiploid/ / BWL4444	T	2.81*	2.96*	2.1*	1.85*	1.62*	2.84**	2.11*	1.61*	1.81*	1.28*	1.82*	2.08*	1.21*	1.34*	1.26*	2.21*	0.21	2.35*	1.99*	1.63*
	S	1.96*	2.68*	2.07*	1.85*	11.68***	3.67**	1.87***	2.93*	2.29*	1.30*	1.28*	2.01***	2.07***	2.87*	2.04*	1.87*	0.38	1.44*	2.23**	1.63*
	G x T	2.03*	2.33*	1.99*	2.28*	2.15*	1.89*	1.55***	1.45***	1.98***	1.49***	1.66***	1.83***	1.81***	3.95*	1.22*	1.98*	1.08	1.09*	1.27*	1.23*
	G x S	206*	3.07*	1.98*	2.67**	3.03**	3.72**	2.45*	1.21*	1.33*	2.83*	2.81**	2.33*	1.29*	1.99*	2.97*	2.87*	0.87	2.83**	1.64*	1.84*
	T x S	1.50*	3.46**	3.68*	1.64*	1.72*	1.61*	1.27*	2.36*	3.2*	2.02*	1.44*	2.03*	2.05*	2.82*	2.99*	1.63*	1.33	1.55*	1.57*	1.99*
	G x T x S	3.01*	2.98*	2.78*	2.94**	2.97*	1.74*	2.46*	2.77*	2.65*	2.79*	1.80*	2.25*	2.27*	2.91*	1.73*	2.62*	0.62	1.65*	1.76*	1.75*

*significant at <0.05 level, **significant at <0.01 level, ***significant at <0.001 level

Table 3 The significant marker-trait associations and putative candidate genes identified across different treatments for the NUE related, root, plant morphological, yield and yield related traits in a genome wide association study conducted on nested synthetic wheat introgression libraries

SNP	Chr	Position (bp)	Trt/Trait	*p*-value	R^2	FDR	Gene stable ID	Gene end (bp)	Gene start (bp)	Description	Function
AX-95136668	3A	690432670	N60, N120 (GY)	5.85E-07	0.202	0.001	TraesCS3A02G452300	690460596	690459736	flowering-promoting factor 1-like protein 2	regulates flowering (Kania et al. 1997) and gibberellin signalling pathway
AX-94415776	6A	28700804	N60, N120 (GY)	1.54E-06	0.2	0.001	ENSRNA050010223	28845847	28845775		
AX-94978974	6A	29876500	N60, N120 (GY)	1.20E-06	0.202	0.001	TraesCS6A02G056800	29879453	29877038	putative disease resistance protein At3g14460	defence response to fungus (Bianchet et al. 2019)
AX-94737868	6A	29876631	N60, N120 (GY)	6.07E-07	0.204	0.001					
AX-95210745	6A	29967076	N60, N120 (GY)	1.27E-06	0.202	0.001	TraesCS6A02G057000	29969466	29967087	putative F-box protein At3g16210	regulates gibberellin signalling (McGinnis 2003); panicle and seed development in rice (Jain et al. 2007, Li et al. 2011)
AX-95631197	6A	30030973	N60, N120 (GY)	5.94E-07	0.206	0.001	TraesCS6A02G057100	30036467	30032329	F-box protein At5g03970-like	APO gene in rice improved grain yield per plant (Terao et al. 2010)
AX-95011132	6A	30031026	N60, N120 (GY)	7.51E-07	0.202	0.001					
AX-95255669	6A	30873212	N60, N120 (GY)	8.32E-07	0.202	0.001	TraesCS6A02G058500	30876811	30873143	L-type lectin-domain containing receptor kinase IX.1	promotes cell death (Wang et al. 2015), resistance response to pathogens (Wang et al. 2014)
AX-95219967	6A	31036496	N60, N120 (GY)	1.11E-06	0.201	0.001	TraesCS6A02G058700	31036808	31034388	LURP-one-like protein (DUF567)	defence and resistance to *H. parasitica* mediated by the R-proteins RPP4 and RPP5 (Gallego-Giraldo et al. 2018)
AX-95070275	6A	31048271	N60, N120 (GY)	7.49E-07	0.204	0.001					
AX-94970334	6A	31474354	N60, N120 (GY)	1.30E-06	0.199	0.001					
AX-94894393	6A	34032797	N60, N120 (GY)	8.00E-07	0.201	0.001	TraesCS6A02G063700	34033068	34029127	F-box protein At5g03970-like	APO gene in rice improved grain yield per plant (Terao et al. 2010)
AX-95249202	6A	34285660	N60, N120 (GY)	8.46E-07	0.199	0.001	TraesCS6A02G064600	34285946	34283159	predicted protein	
AX-94553503	6A	34982713	N60, N120 (GY)	8.83E-07	0.201	0.001	TraesCS6A02G065400	34983010	34979092	serine/arginine-rich splicing factor RS41 isoform X2	abiotic stress tolerance (Palusa et al. 2007)

AX-94696366	6A	35482343	N60, N120 (GY)	7.06E-07	0.201	0.001	TraesCS6A02G066200	35484242	35478280	protein accumulation and replication of chloroplasts 6, chloroplastic	chloroplast division (Zhang et al. 2015), regulation of mitochondrial DNA replication as well as gene transcription and translation (Tang et al. 2019)
AX-94386201	6A	35580470	N60, N120 (GY)	7.83E-07	0.2	0.001	TraesCS6A02G066800	35581719	35580136	transcription termination factor MTERF4, chloroplastic-like	chloroplast or mitochondria development (Quesada 2016)
AX-94835065	6A	36106101	N60, N120 (GY)	1.46E-06	0.197	0.001	TraesCS6A02G067700	36110655	36105754	S-(+)-linalool synthase, chloroplastic-like	monoterpene (C10) biosynthesis, resistance to the bacterial blight pathogen *Xanthomonas oryzae* pv. *oryzae* (Taniguchi et al. 2013)
AX-94914391	6A	36429885	N60, N120 (GY)	1.17E-06	0.202	0.001	TraesCS6A02G068000	36433862	36429712	putative HVA22-like protein g	role in stress response (Brands and Ho, 2002), auxin transport to root tips (Janiak et al. 2017)
AX-94606161	6A	64319129	N60, N120 (GY)	1.37E-06	0.203	0.001	TraesCS6A02G097200	64320738	64317228	phosphatidylinositol/phosphatidylcholine transfer protein SFH12-like	transport of secretory proteins from the Golgi complex (Mo et al. 2007)
AX-95072891	6A	690432617	N60, N120 (GY)	1.47E-06	0.201	0.001					
AX-94511241	6B	30282005	N60, N120 (GY)	1.80E-06	0.202	0.001	TraesCS6B02G050900	30281705	30276637	protein STRUBBELIG-RECEPTOR FAMILY 5-like	control male-sterility, organ development, cell proliferation in *Arabidopsis* (Chevalier et al. 2005)
AX-94387975	6B	34398171	N60, N120 (GY)	3.60E-06	0.191	0.001	TraesCS6B02G054200	34341419	34340169	papain-like cysteine proteinase	up-regulation of multiple pathogenesis-related proteins and biosynthesis of secondary metabolites (Niño et al. 2020), proteolysis and physiological processes (Liu et al. 2018)
AX-94511284	6B	51737371	N60, N120 (GY)	1.92E-06	0.202	0.001	TraesCS6B02G075400	51736016	51732081	F-box protein At5g03970-like	APO gene in rice improved grain yield per plant (Terao et al. 2010)
AX-94816913	6B	64929420	N60, N120 (GY)	1.33E-06	0.2	0.001	TraesCS6B02G089500	64929918	64925602	F-box protein At5g03970-like	APO gene in rice improved grain yield per plant (Terao et al. 2010)

AX-94607905	2A	571213772	N0, (DSW); N120 (DRW, DSW)	9.13E-07	0.199	0.001	TraesCS2A02G337700	571150423	571149635	non-specific lipid-transfer protein-like protein At2g13820	lipid binding and transport, xylem differentiation (Motose et al. 2004, Kobayashi et al. 2011)
AX-94923560	2A	729858414	N60 (FRW, DRW, FSW, DSW)	1.95E-06	0.128	0.001	TraesCS2A02G501900	729858636	729852393	predicted protein	
AX-94705680	2B	598802253	N120 (DRW); N60 (FSW)	1.29E-06	0.198	0.001	TraesCS2B02G418100	598959096	598956372	acyl-coenzyme A thioesterase 13	acyl-CoA hydrolase activity (Cheng et al. 2006); improves grain filling rate in rice (Zhao et al. 2019); lipid metabolism
AX-95203088	2B	613322090	N60 (FSW, DSW); N120 (DRW, DSW)	1.72E-06	0.194	0.001	TraesCS2B02G426600	613234917	613205484	subtilisin-like protease SBT1.7	seed coat development and mucilage release (Rautengarten et al. 2008)
AX-94601746	2B	743105753	N60 (FSW), N120 (DRW)	4.85E-07	0.203	0	TraesCS2B02G546300	743331453	743328441	unnamed protein product	
AX-94887553	2D	580238575	N0 (FSW, DSW); N60 FRW, DRW, DSW); N120 (DRW, FSW)	6.41E-07	0.137	0.001	TraesCS2D02G479500	580238874	580235096	Protein CutA 1, chloroplastic	Cadmium content and leaf margin trait (https://www.uniprot.org/uniprot/Q109R6), copper ion binding (Burkhead et al. 2003).; signal transduction (Arnesano et al. 2003); nitrogen regulatory response in bacterial and eukaryotic chloroplast (Ninfa and Atkinson, 2000, Arcondéguy et al. 2001)
AX-94735141	2D	581570385	N60 (DRW, DSW, FSW); N120 (FRW, DRW, FSW, DSW)	2.32E-06	0.127	0.001	TraesCS2D02G480200	581526532	581523421	unnamed protein product	
AX-94474729	2D	584545802	N60 (FRW, DRW)	1.82E-06	0.13	0.001	TraesCS2D02G481800	584545905	584542725	Anthocyanidin reductase	oxidoreductase activity and flavonoid biosynthetic process (Winkel-Shirley, 2001)
AX-94835810	2D	584799948	N0 (DRW, FSW, DSW); N60 (DRW, DSW); N120 (DRW, FSW, DSW)	2.69E-06	0.175	0.002	TraesCS2D02G482500	584804705	584799573	predicted protein	
AX-95223893	2D	584861391	N0 (FRW, DRW, FSW, DSW), N60 (DRW, DSW,	3.55E-07	0.186	0.002	TraesCS2D02G482800	584864531	584861189	tRNA (guanine(10)-N2)-methyltransferase homolog	tRNA modification, drought, salt and cold stress 'response, root and plant development in rice

			FSW); N120 (FRW, DRW, FSW, DSW)							and Arabidopsis (Wang et al. 2017)
AX-95003296	2D	586331032	N0 (FSW, DSW); N60 (FRW, DRW)	1.49E-06	0.129	0.001	TraesCS2D02G485600	586331902	586329940	unnamed protein product	
AX-94477325	2D	586572446	N0 (DRW, FSW, DSW); N60 (FRW, DRW); N120 (DRW)	2.80E-06	0.174	0.002	TraesCS2D02G486000	586575253	586571354	uncharacterized protein LOC109744903	
AX-95197137	2D	586839201	N0 (FSW, DSW); N60 (FRW, DRW); N120 (DRW, FSW)	7.71E-07	0.133	0.001	TraesCS2D02G486400	586846982	586841634	receptor-like serine/threonine-protein kinase SD1-8	regulation of cellular expansion and differentiation in Arabidopsis, ATP and carbohydrate binding, defence and signalling (Uniprot)
AX-94525577	2D	587107149	N0 (FSW, DSW), N60 (FRW, DRW); N120 (FSW)	3.71E-07	0.137	0.001	TraesCS2D02G487000	587107595	587106896	predicted protein	
AX-94702180	2D	587292781	N0(FSW, DSW); N60(FRW, DRW)	5.41E-07	0.136	0.001	TraesCS2D02G487700	587293147	587282608	putative kinesin motor domain-containing protein	regulate rice seed length (Kitagawa et al. 2010); male meiosis, anther dehiscence, and fertility in rice (Zhou et al. 2011)
AX-94487982	2D	588675894	N0 (FSW, DSW); N60 (FRW, DRW); N120 (DRW, FSW)	3.34E-07	0.173	0	TraesCS2D02G489700	588677693	588676152	WRKY45-like transcription factor	regulates Pi uptake by modulating PHT1;1 expression in Arabidopsis (Wang et al. 2014); age-triggered leaf senescence (Chen et al. 2017); Benzothiadiazole-inducible blast resistance (Shimono et al. 2007); resistance against *F. graminearum* in wheat (Bahrini et al. 2011); broad-spectrum resistance to wheat powdery mildew (Cao et al. 2011)
AX-95190381	2D	591027900	N0 (FSW, DSW); N60 (FRW, DRW); N120 (DRW, FSW)	2.11E-07	0.18	0	TraesCS2D02G493700	591031752	591027189	serine-threonine protein kinase	regulates stress-responsive gene expression in rice (Diédhiou et al. 2008), Negative regulator of immune responses in Arabidopsis (Lin et al. 2015); confers durable and broad-spectrum resistance to wheat

											powdery mildew (Cao et al. 2011)
AX-95018936	2D	595159320	N60 (DRW); N120 (DRW, DSW)	3.19E-06	0.126	0.001	TraesCS2D02G500500	595161251	595157820	JmjC domain-containing protein	regulation of RNA silencing, DNA methylation (Qian et al. 2019), Brassinosteroid (BR) signalling pathway, affecting flowering, and biorhythm and bud regeneration (Yokoo et al. 2014)
AX-94457170	2D	596252217	N0 (DSW); N120 (FSW)	2.41E-06	0.164	0.001	TraesCS2D02G502700	596252069	596254635	Adenine nucleotide alpha hydrolases-like superfamily protein	hydrolase activity and root hair cell differentiation (https://www.uniprot.org/uniprot/Q84JS5); response to salt stress (Jung et al. 2015); involved in male sterility (Mok and Mok 2001)
AX-94962360	2D	596914793	N0 (DRW, FSW, DSW); N60 (FRW, DRW, DSW); N120 (FSW)	4.51E-07	0.185	0.002	TraesCS2D02G503000	596917719	596911132	plasma membrane H^+-ATPase	Plant adaptation to environmental stresses (Janicka-Russak and Kabala, 2015), P deficiency and Al toxicity (Yu et al. 2015, Wang et al. 2014), transport of various nutrients (nitrate, phosphate and potassium) through roots, elongation of hypocotyls in Arabidopsis (Takahashi et al. 2012); NH_4^+ metabolism in rice roots (Weng et al. 2020); auxin-mediated cell elongation during wheat embryo development (Rober-Kleber 2003)
AX-94829391	2D	601212171	N0 (DSW); N60 (DRW)	1.84E-06	0.128	0.001	TraesCS2D02G507800	601215051	601211912	Nuclease S1	nucleic acid degradation during plant programmed cell death (Lesniewicz et al. 2013)
AX-94786006	2D	610277424	N60 (FRW, DRW, FSW); N120 (FRW)	1.13E-06	0.131	0.001	TraesCS2D02G521400	610282317	610276851	3-oxoacyl-[acyl-carrier-protein] synthase III, chloroplastic	fatty acid biosynthesis and metabolism, lipid biosynthesis and metabolism (https://www.uniprot.org/uniprot

											/P49243), role in rice root development (Ding et al. 2015)
AX-94695716	2D	702726797	N60 (FSW, DSW); N120 (FRW, DRW, DSW)	2.82E-06	0.193	0.002					
AX-95136655	3B	234490336	N0, N60, N120 (DTF)	1.70E-06	0.161	0.016	TraesCS3B02G201300	233224384	233224014	protein DEHYDRATION-INDUCED 19-like	drought tolerance in rice (Wang et al. 2014) and Arabidopsis through up-regulation of pathogenesis-related PR1, PR2, and PR5 gene expressions (Liu et al. 2013); response to salt and water stress (https://www.uniprot.org/uniprot/Q84J70), accelerate flowering (Hwang et al. 2019)
AX-95113687	6A	595578832	N120 (RSA); N60 (Tips)	3.04E-06	0.256	0.006	TraesCS6A02G371000	595564219	595563589	predicted protein	
AX-94513497	6A	595627899	N0 (RSA, RV); N60 (RSA, RV, Tips); N120 (RSA, RV, Tips)	1.89E-07	0.311	0.001	TraesCS6A02G371300	595628211	595624936	predicted protein	
AX-94911804	6A	595776559	N0 (RSA, RV); N60 (RSA, RV, Tips); N120 (RSA, RV, Tips, Forks)	5.24E-07	0.307	0.002	TraesCS6A02G371800	595778154	595774917	vesicle-associated membrane protein 713	Protein transport, response to salt stress (https://www.uniprot.org/uniprot/Q9LFP1), tolerance to water stress (Singh et al. 2017); growth and immune response in Arabidopsis (Yun et al. 2013)
AX-94565231	6D	683646420	N0 (RSA); N60 (RSA, TRL, RV, Tips); N120 (RSA, RV, Forks, Tips)	8.41E-07	0.305	0.003					
AX-94676800	7A	376797697	N60 (FSW); N120 (DRW)	2.79E-06	0.195	0.001	TraesCS7A02G293700	376870968	376869867	calcium/calmodulin-regulated receptor-like kinase 2	response to cold, plant tolerance to salt and ABA stress (Yang et al. 2010)

p-value: significance level of marker-trait association; R^2: percent phenotypic variance explained by the SNP; FDR: false discovery rate, p-value, R^2 and FDR is represented as the mean value across seasons

Table 4 The top 10 nitrogen insensitive (NIS) and 10 nitrogen sensitive (NS) breeding lines with contrasting grain yield (GY; kg ha^{-1}) derived from pooled mean over two seasons and three treatments

Category	Designation	Pop	Mean GY	2018_N0	2019_N0	2018_N60	2019_N60	2018_N120	2019_N120
NIS	HT661	Pop1	3289	2865	2869	4093	3843	3190	2873
NIS	HT712	Pop1	3237	3145	3568	3435	3458	2902	2915
NIS	HT722	Pop1	3195	3102	3349	3158	3338	2892	3328
NIS	HT726	Pop1	3172	2982	2502	3978	3522	2845	3203
NIS	HT723	Pop1	2970	2802	2791	3207	2930	3222	2867
NIS	HT1913-2	Pop4	2933	2332	2526	2909	2616	3693	3523
NIS	HT1870	Pop4	2911	2122	2433	2632	2745	3665	3871
NIS	HT727	Pop1	2911	2377	1833	3370	3012	3610	3266
NIS	HT1908-2	Pop4	2900	2641	2148	2851	2368	3553	3837
NIS	HT764-1	Pop2	2897	2440	2897	3528	2872	2747	2896
NS	HT1723	Pop3	1885	1158	760	1806	1813	2675	3096
NS	HT696	Pop1	1750	825	1261	1660	1950	2455	2350
NS	HT704	Pop1	1661	827	1245	1948	1274	2297	2372
NS	HT644	Pop1	1658	989	1384	1838	1474	1822	2443
NS	HT845	Pop2	1625	1111	1232	1700	1793	2038	1878
NS	HT1882-3	Pop4	1594	918	1186	1256	1646	1982	2576
NS	HT647	Pop1	1590	846	985	1082	1535	2440	2652
NS	HT765	Pop2	1519	768	1162	1375	1606	1720	2484
NS	HT665	Pop1	1413	542	1010	1187	1077	2370	2292
NS	HT847	Pop2	1359	683	717	1258	1333	1980	2182

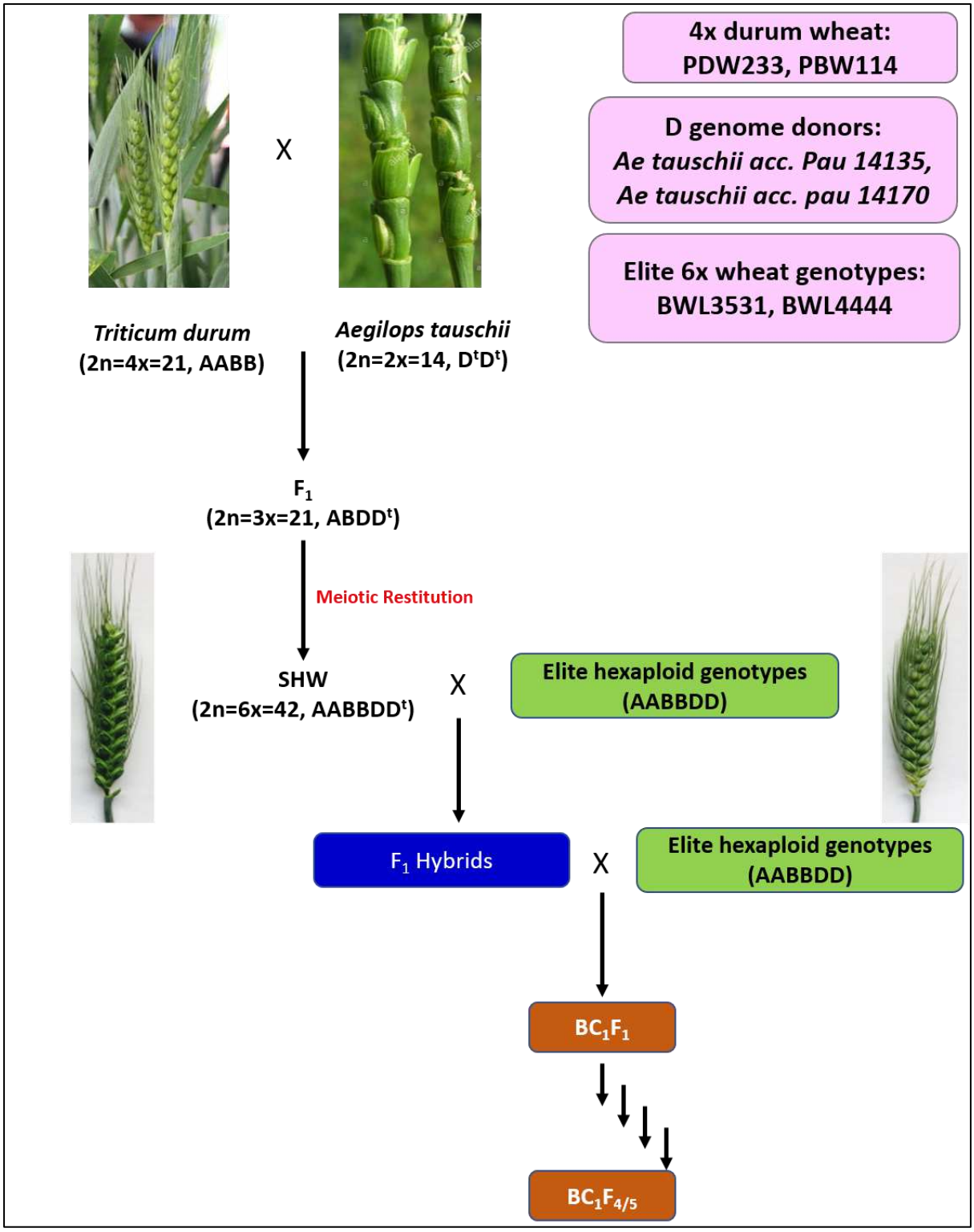

Fig 1. Schematic representation of the breeding strategy used to develop the nested synthetic wheat introgression libraries.

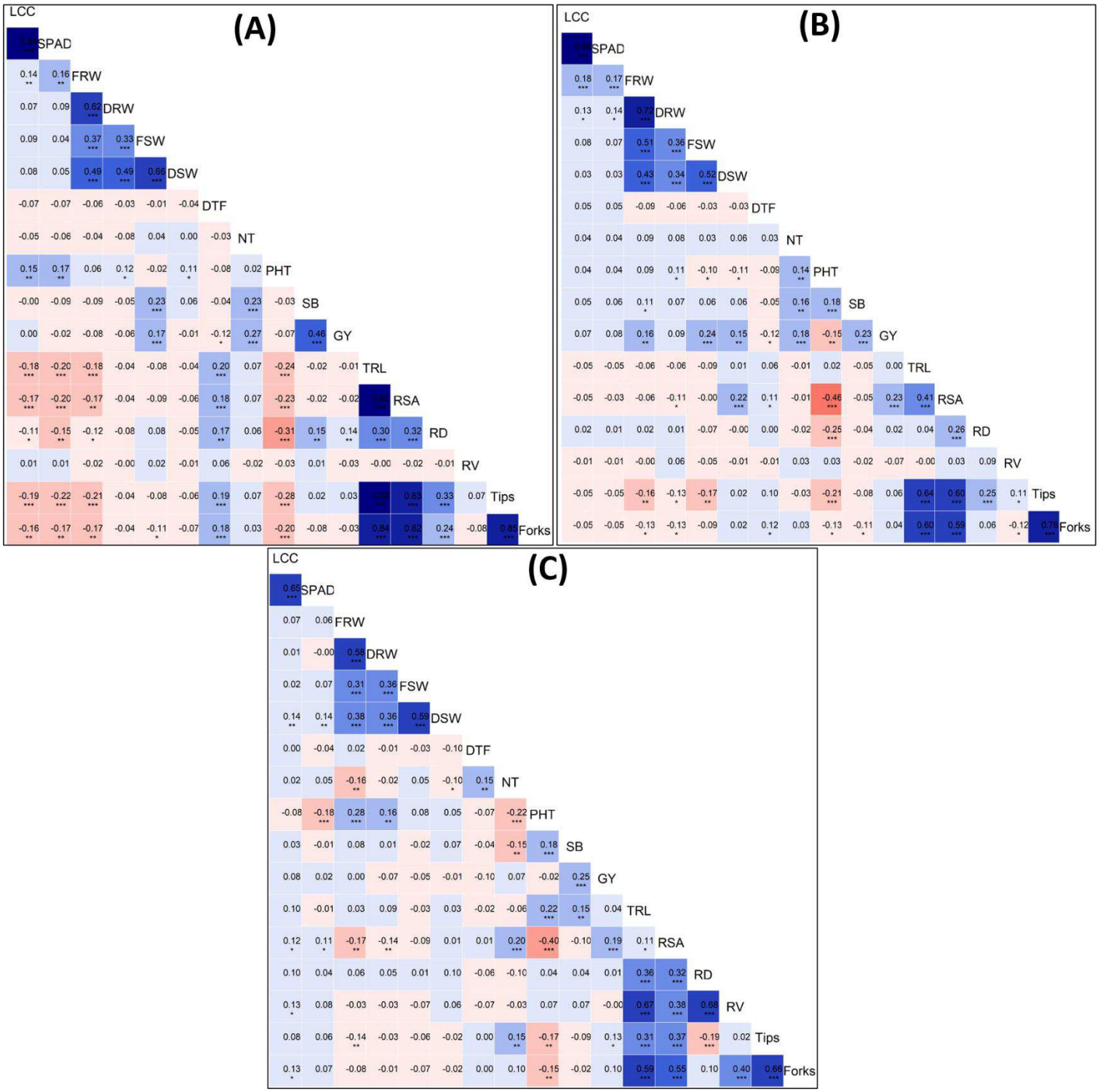

Fig 2. Plots of Pearson's *r-values* showing the correlation among traits measured (A) at N0, (B) N60 and (C) N120 level. The blue colour indicates positive correlation and red colour indicated the negative correlation among different traits, the variation in colour intensity is representing the strength of the correlation among the traits. *significance at <5% level, **significance at <1% level, ***significance at <0.1% level.

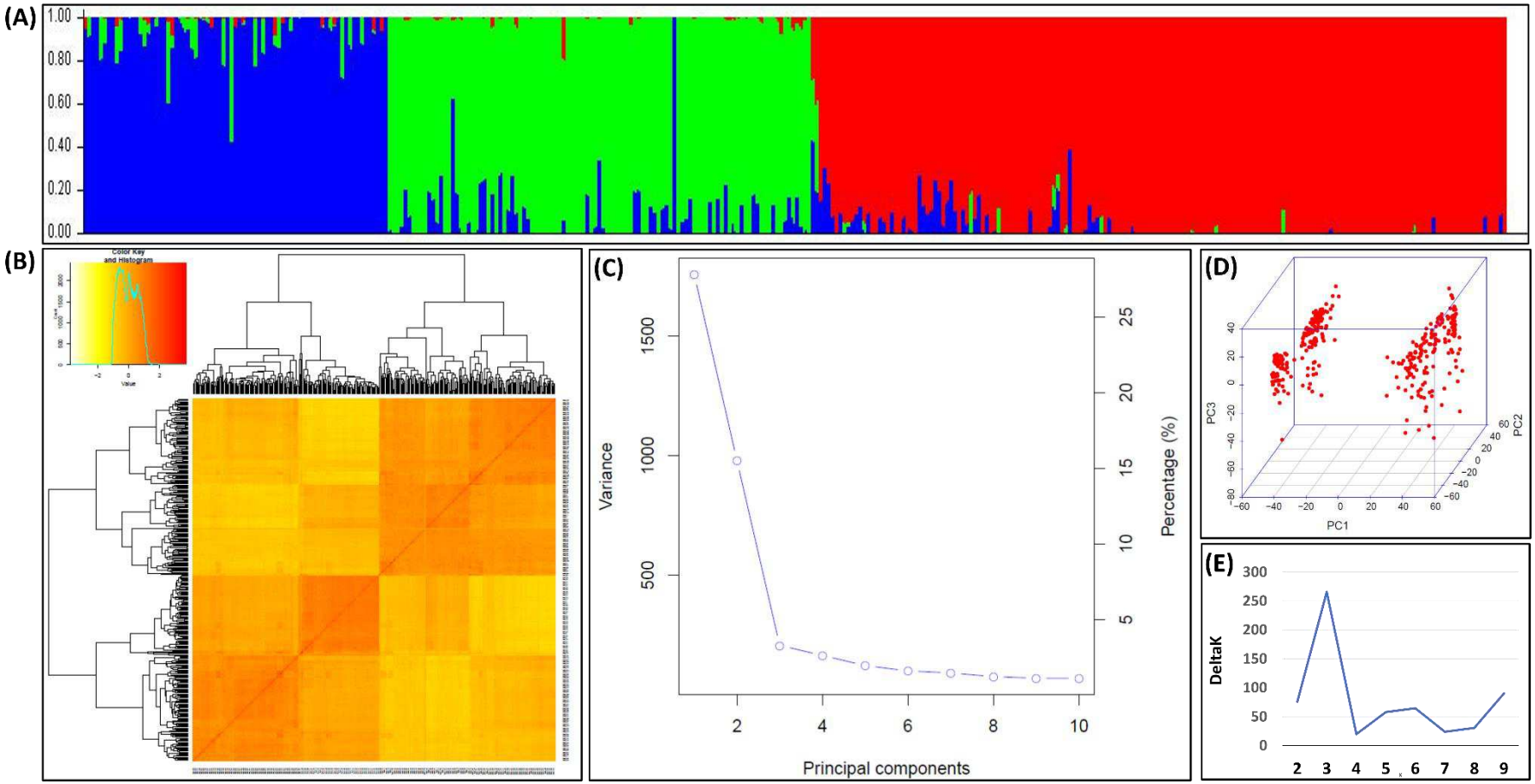

Fig. 3 (A) Population structure within the nested synthetic wheat introgression libraries. The population structure plots with each vertical bar representing a breeding line coloured according to the particular group to which the breeding line has been assigned. The breeding lines assigned to more than one of group represents the degree of their admixed set of the alleles. (B) The Kinship matrix displayed as the heat map, where the red indicates the highest correlation between the pairs of breeding lines and yellow indicates the lowest correlation. (C) The Scree plot indicating the most of the variability explained by first three PCs for association study. (D) The three-dimensional view of the principal components explaining the genotypic variation among breeding lines constituting the introgression libraries (E) The appropriate number of the sub-populations determined from the largest *delta K*=3

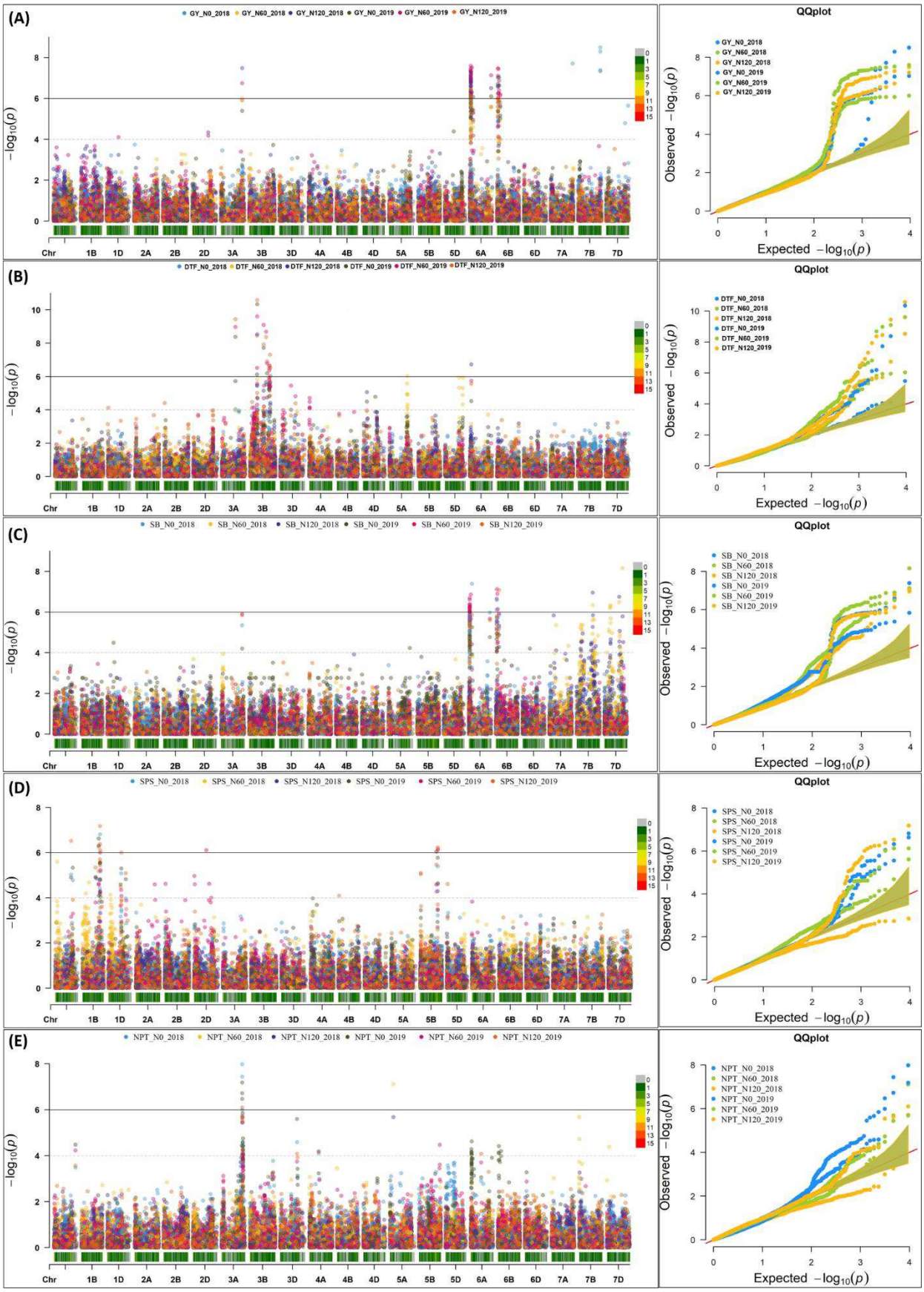

Fig. 4 Manhattan plot and qq plot for the yield and yield related traits across seasons at three differential level of nitrogen (N0, N60, N120) (A) grain yield (GY) (B) Days to 50% flowering (DTF) (C) shoot biomass (SB) (D) spikelets per spike (SPS) and (E) number of productive tillers

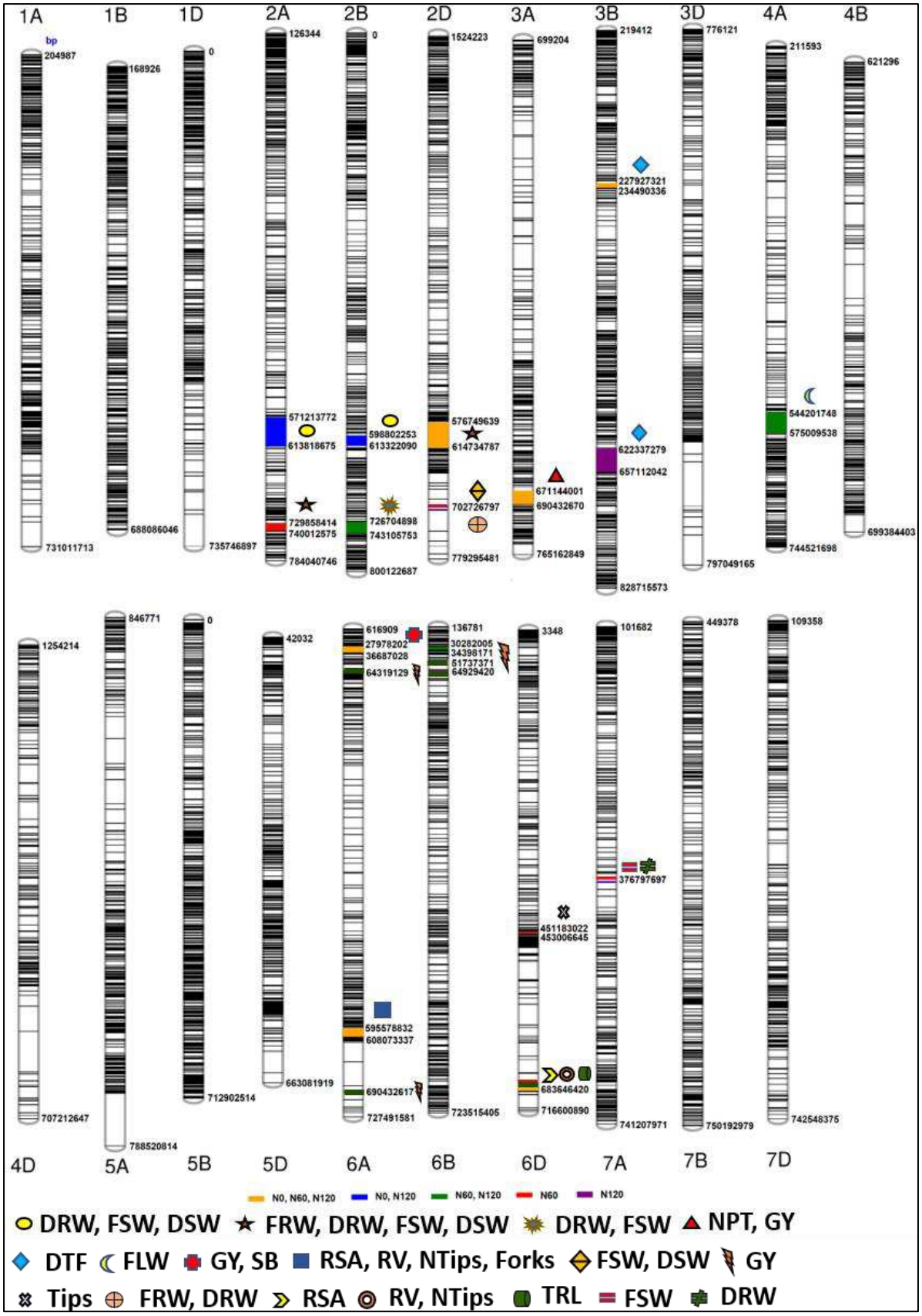

Fig 5 Schematic representation of the SNP distribution along the 21 chromosomes of wheat. The chromosome map showing genomic regions where MTAs for different NUE related trait, root traits, yield and yield related traits. The numbers below each chromosome indicate chromosome numbers. The bp representing the physical position of the SNPs on the chromosome in base pair.

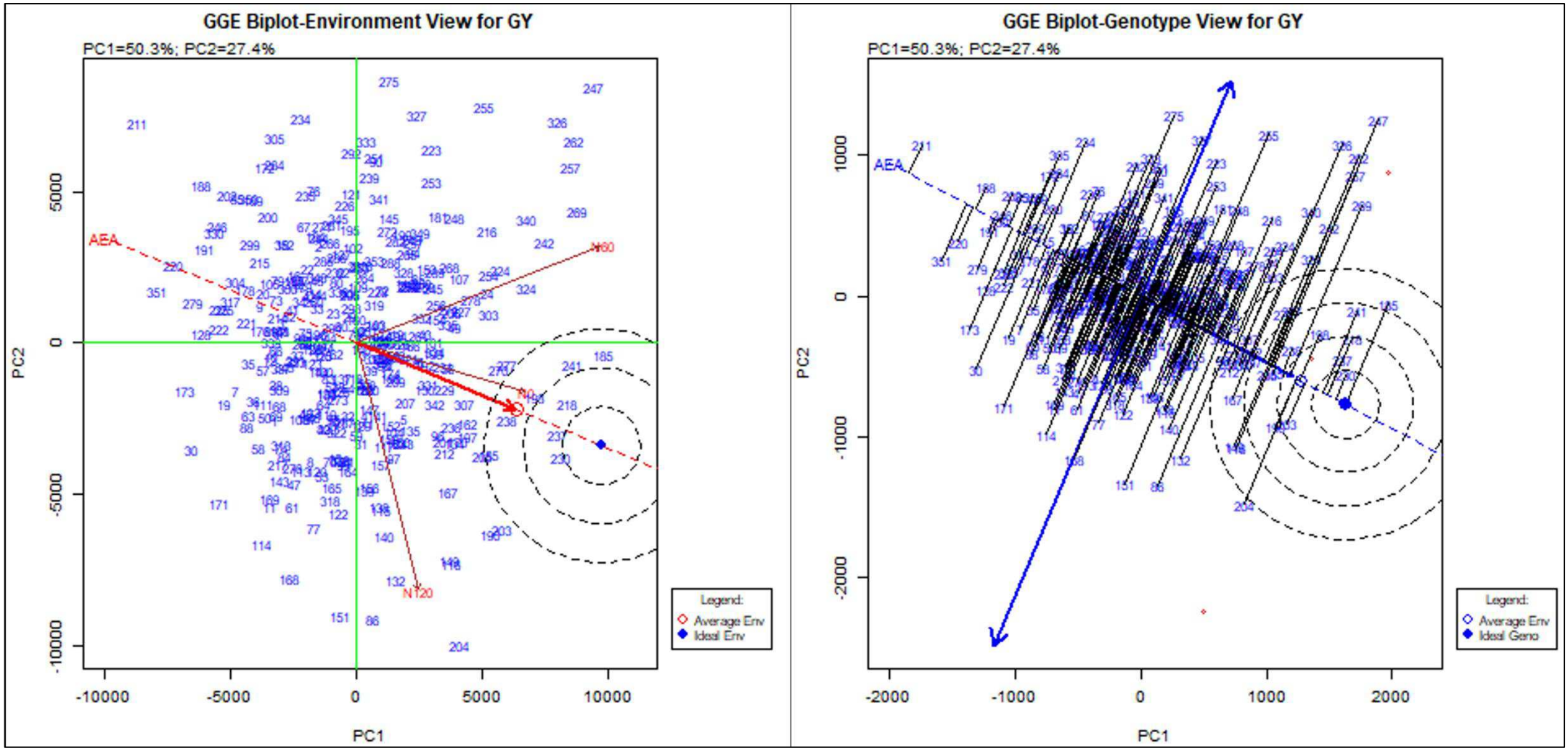

Fig. 6 GGE biplot showing the performance of 352 nested synthetic wheat introgression lines across seasons and treatments (N0, N60, N120). The environment view refers to the three-differential level of nitrogen application: N0, N60 and N120. The genotype view refers to the 352 nested synthetic wheat introgression lines. The numeric number refers to the coding for the introgression lines, which is given in detail in Supplementary table S7.

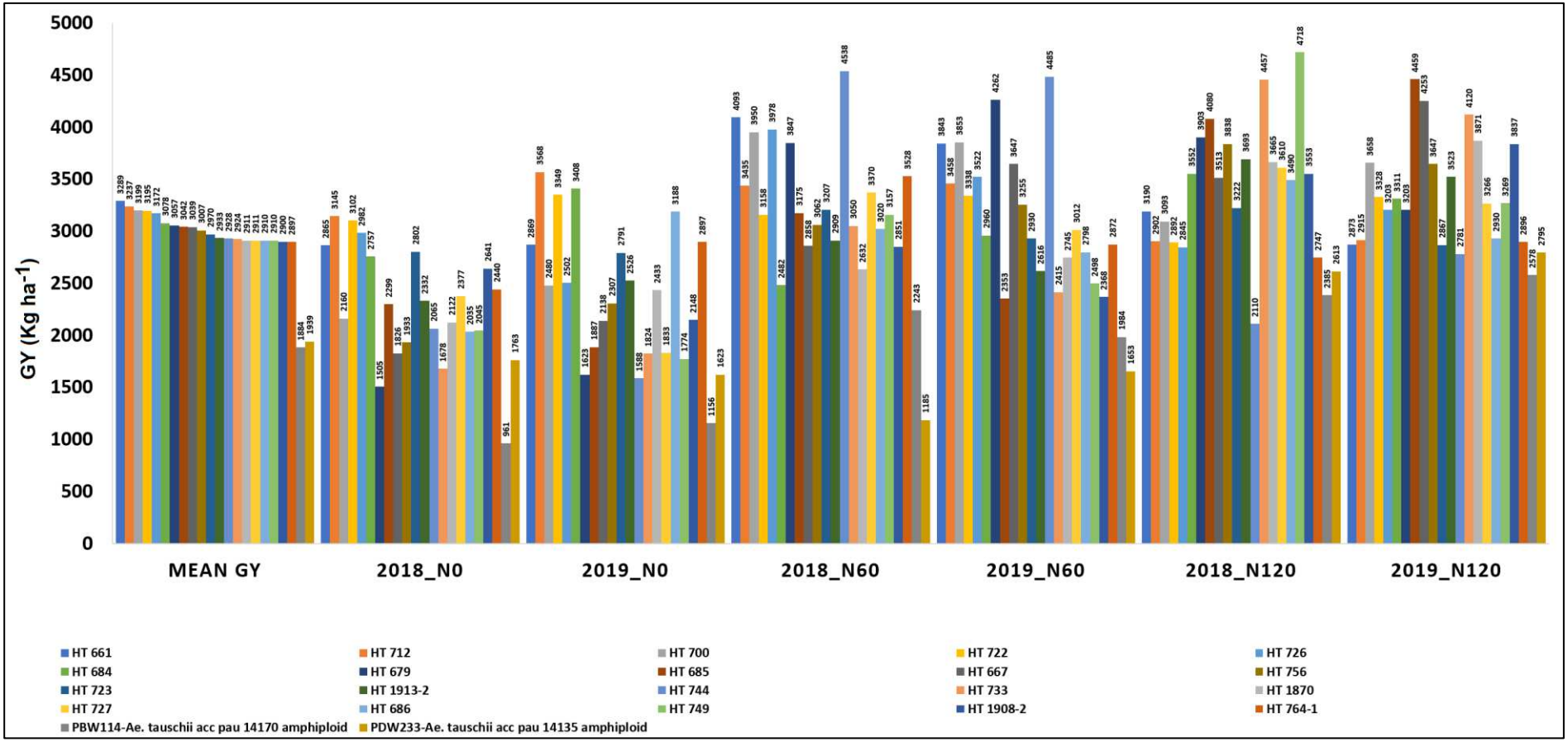

Fig. 7: The grain yield performance of top 20 breeding lines derived from the nested introgression libraries possessing high and stable grain yield (GY; kg ha^{-1}) across two seasons and three treatments. The numeric values above the bar graph indicate the mean grain yield (GY; kg ha^{-1}) performance of breeding lines across seasons.

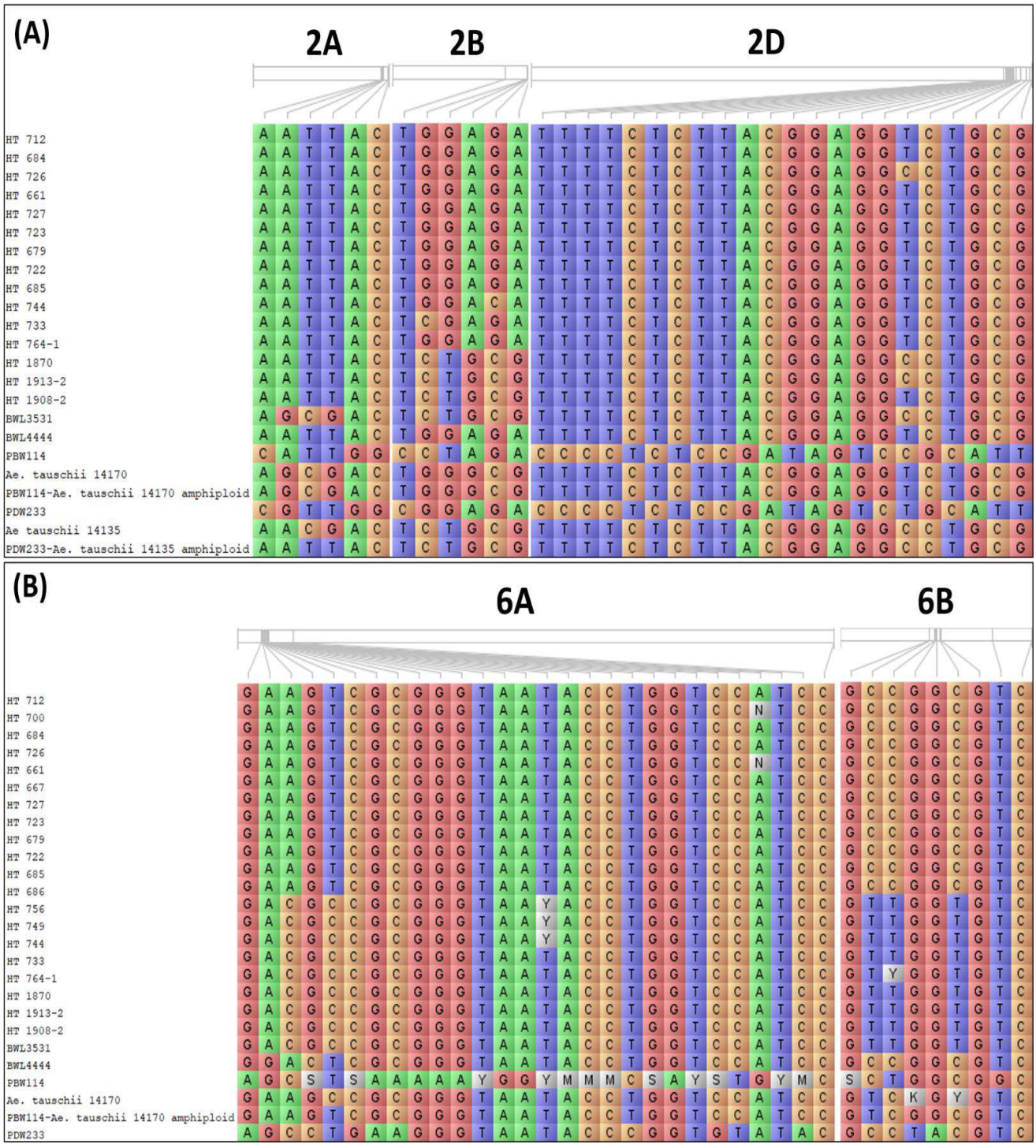

Fig. 8 The allelic constitution of the selected promising breeding lines, wild accessions of *Ae. tauschii*, cultivated and synthetic wheats for the (A) root related traits and (B) grain yield

Figures

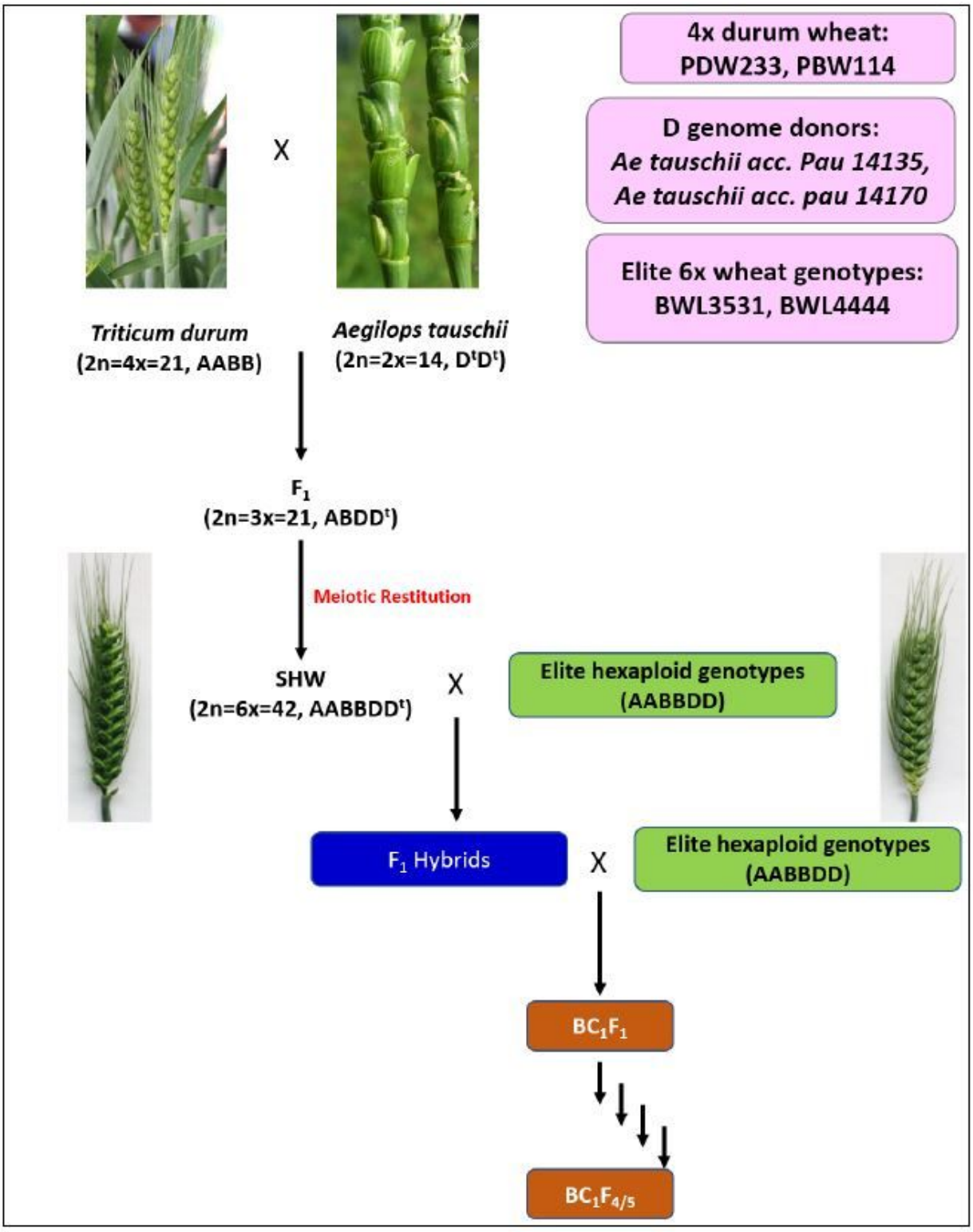

Figure 1

Schematic representation of the breeding strategy used to develop the nested synthetic wheat introgression libraries.

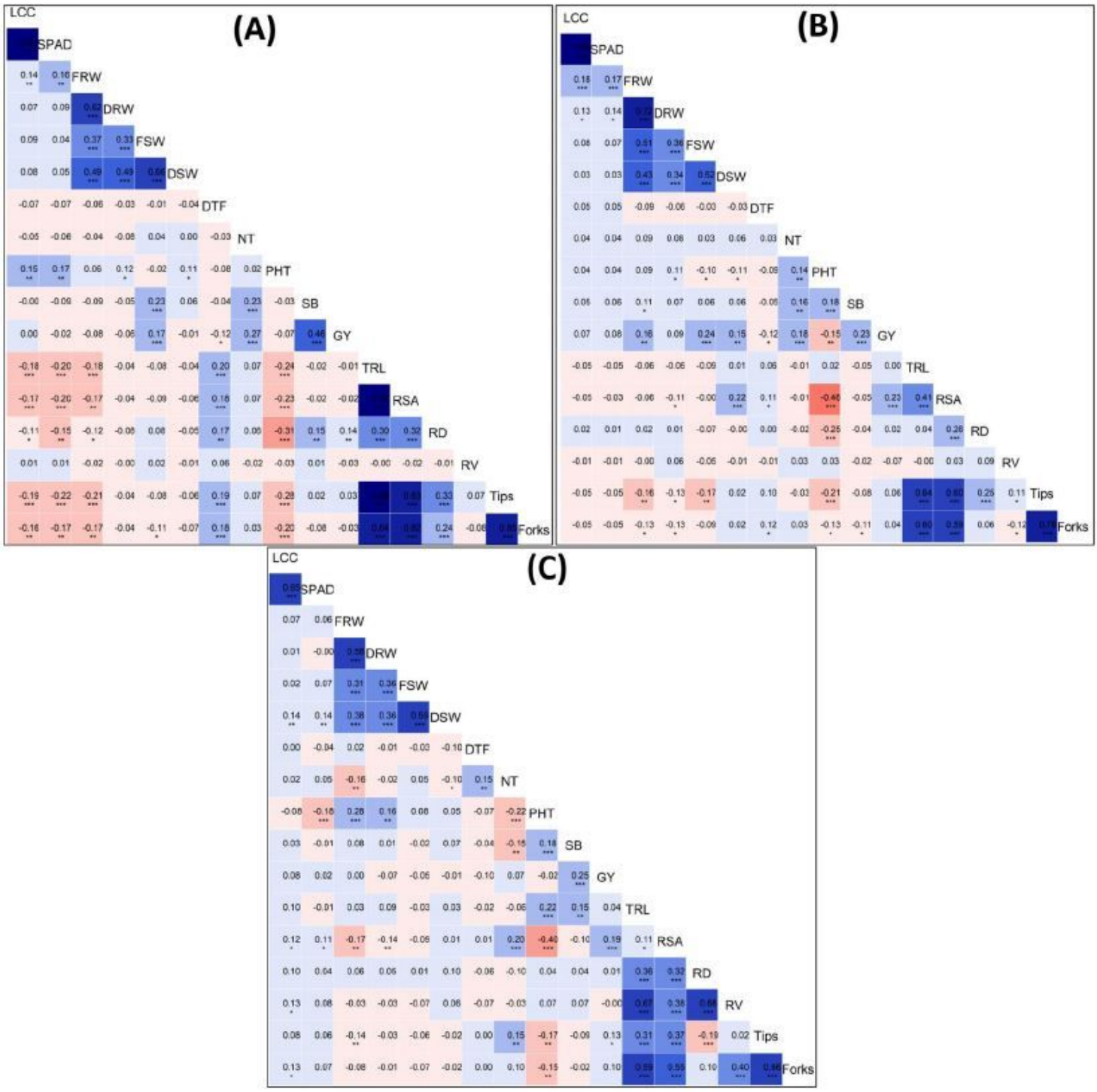

Figure 2

Plots of Pearson's r-values showing the correlation among traits measured (A) at N0, (B) N60 and (C) N120 level. The blue colour indicates positive correlation and red colour indicated the negative correlation among different traits, the variation in colour intensity is representing the strength of the correlation among the traits. *significance at <5% level, **significance at <1% level, ***significance at <0.1% level.

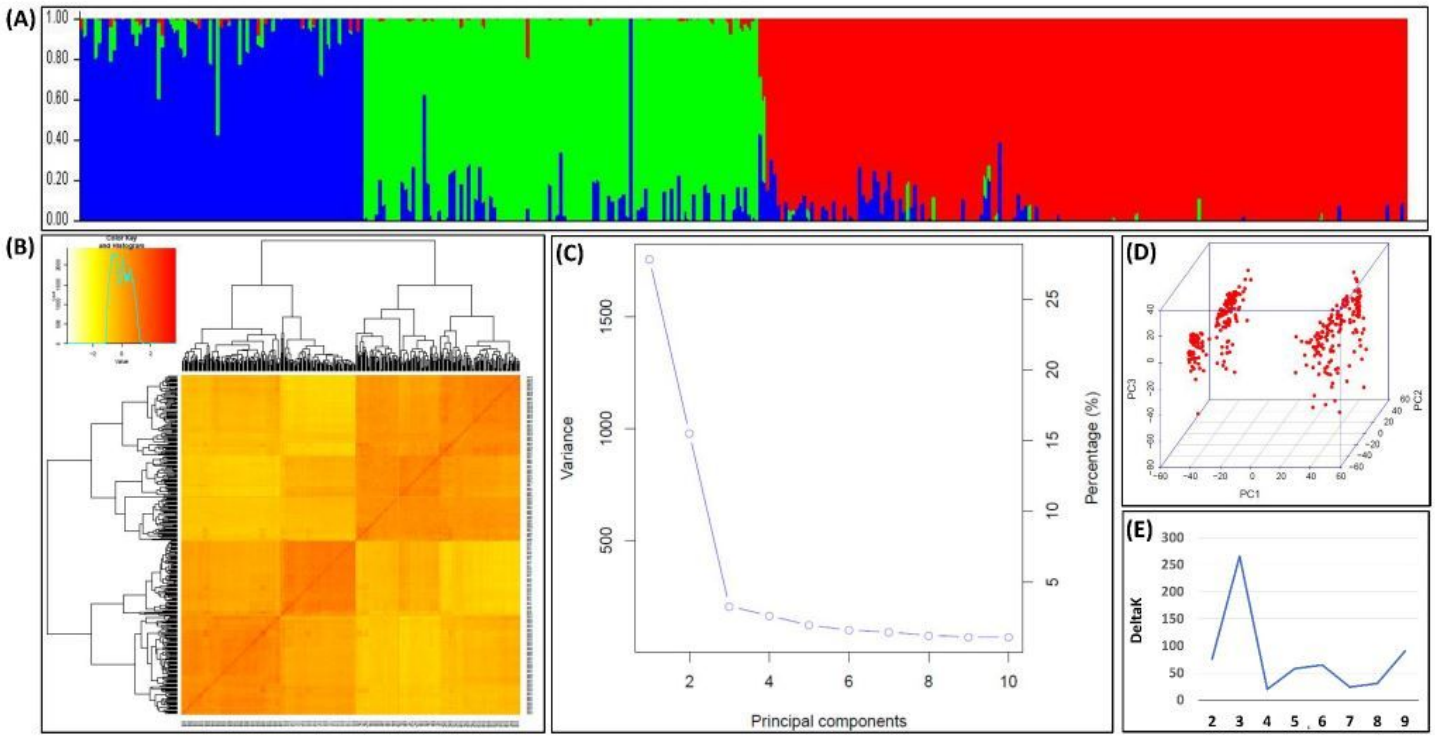

Figure 3

(A) Population structure within the nested synthetic wheat introgression libraries. The population structure plots with each vertical bar representing a breeding line coloured according to the particular group to which the breeding line has been assigned. The breeding lines assigned to more than one of group represents the degree of their admixed set of the alleles. (B) The Kinship matrix displayed as the heat map, where the red indicates the highest correlation between the pairs of breeding lines and yellow indicates the lowest correlation. (C) The Scree plot indicating the most of the variability explained by first three PCs for association study. (D) The three-dimensional view of the principal components explaining the genotypic variation among breeding lines constituting the introgression libraries (E) The appropriate number of the sub-populations determined from the largest delta K=3

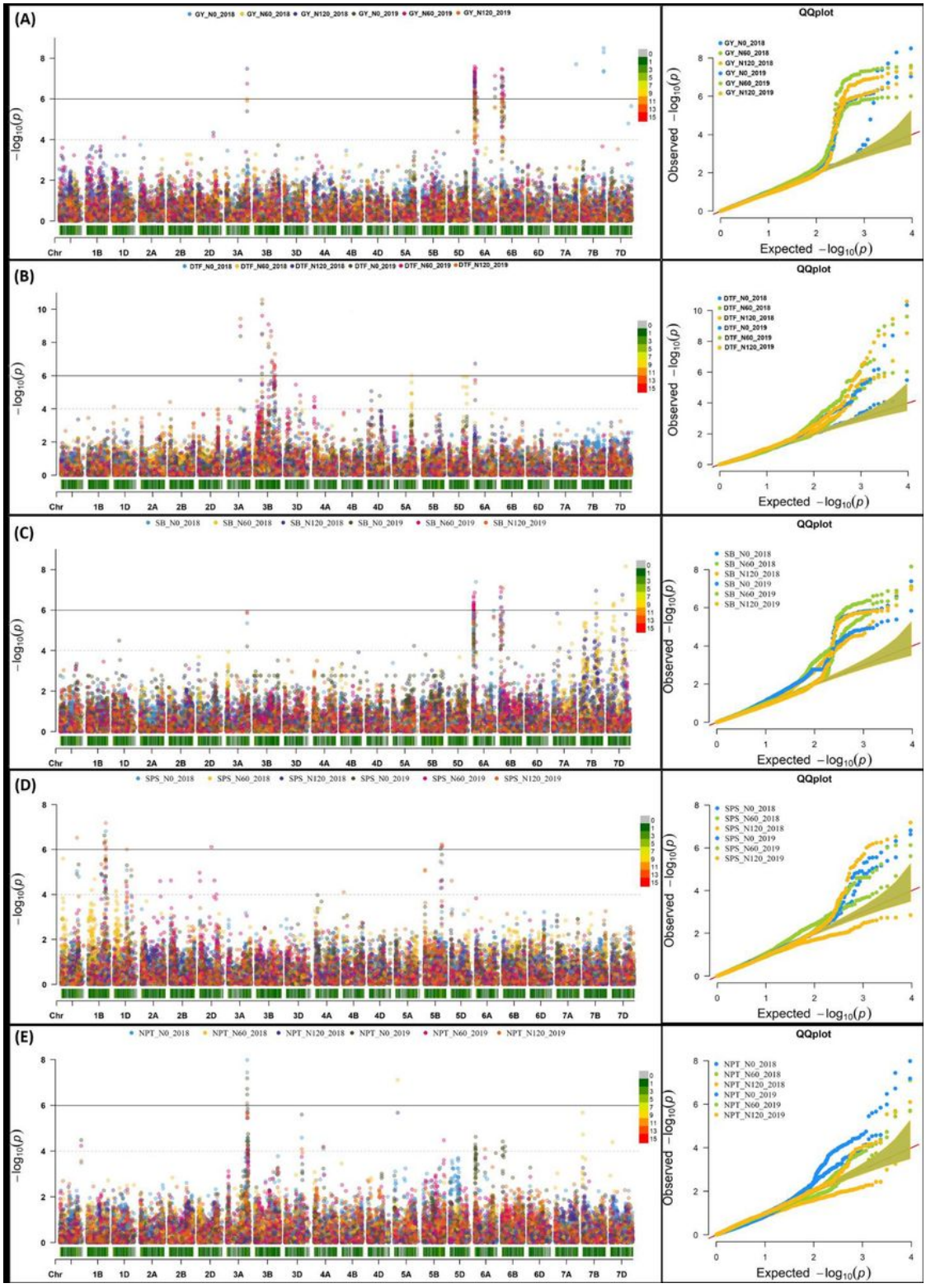

Figure 4

Manhattan plot and qq plot for the yield and yield related traits across seasons at three differential level of nitrogen (N0, N60, N120) (A) grain yield (GY) (B) Days to 50% flowering (DTF) (C) shoot biomass (SB) (D) spikelets per spike (SPS) and (E) number of productive tillers

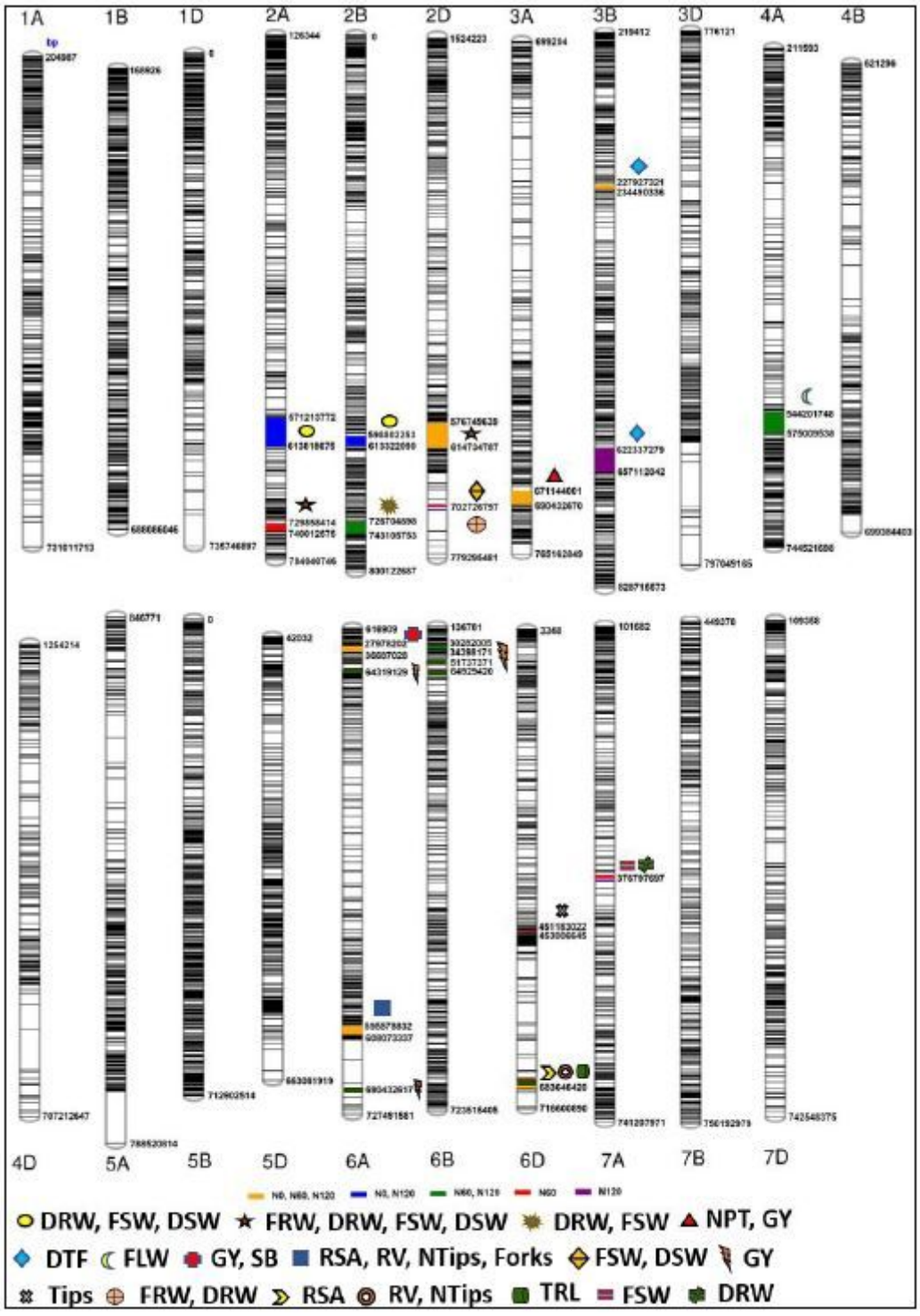

Figure 5

Schematic representation of the SNP distribution along the 21 chromosomes of wheat. The chromosome map showing genomic regions where MTAs for different NUE related trait, root traits, yield and yield related traits. The numbers below each chromosome indicate chromosome numbers. The bp representing the physical position of the SNPs on the chromosome in base pair.

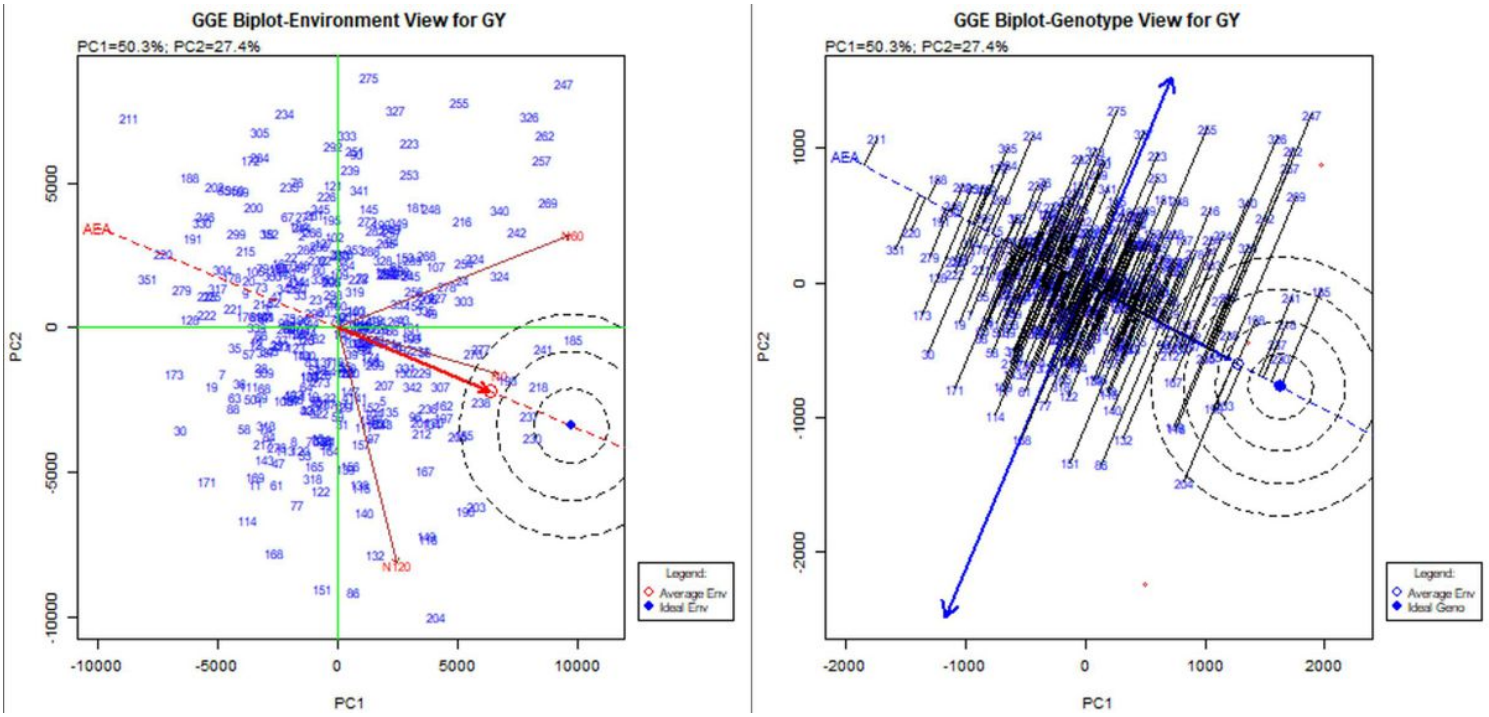

Figure 6

GGE biplot showing the performance of 352 nested synthetic wheat introgression lines across seasons and treatments (N0, N60, N120). The environment view refers to the three-differential level of nitrogen application: N0, N60 and N120. The genotype view refers to the 352 nested synthetic wheat introgression lines. The numeric number refers to the coding for the introgression lines, which is given in detail in Supplementary table S7.

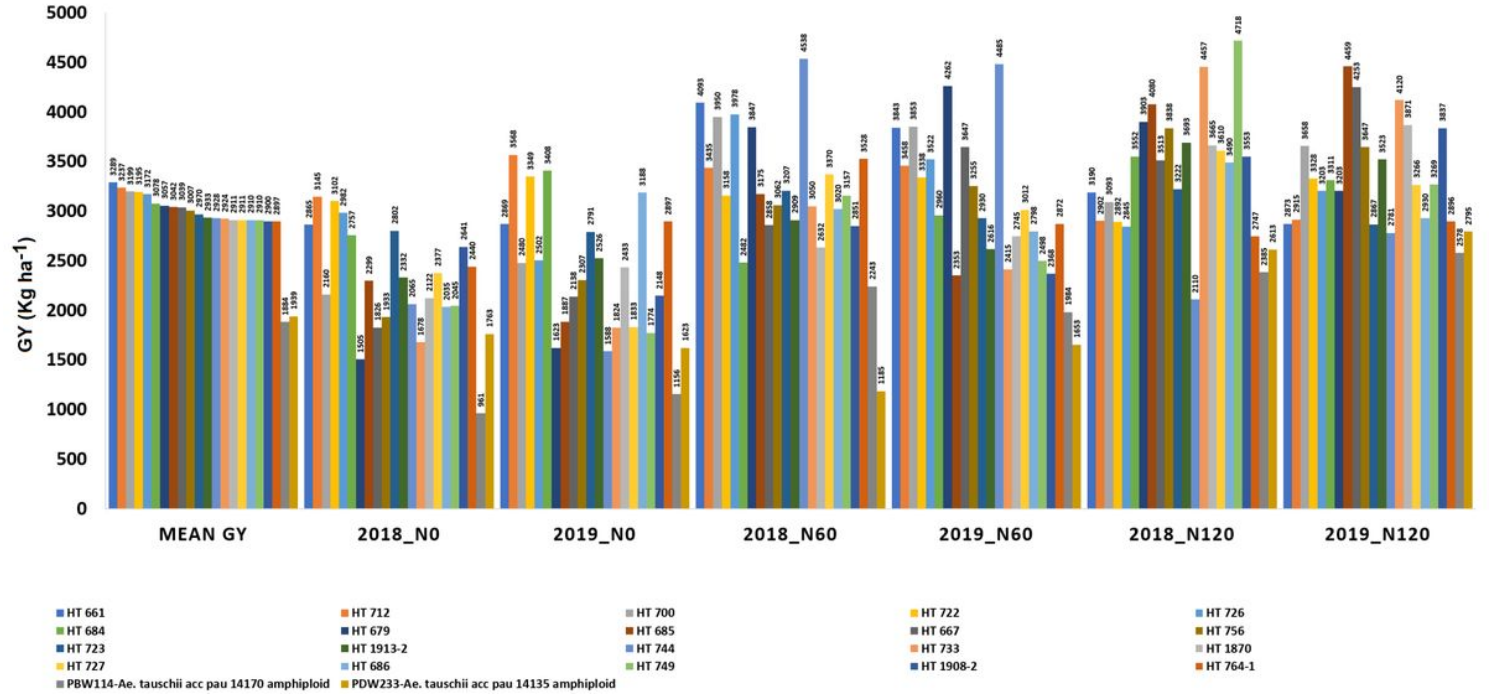

Figure 7

The grain yield performance of top 20 breeding lines derived from the nested introgression libraries possessing high and stable grain yield (GY; kg ha-1) across two seasons and three treatments. The numeric values above the bar graph indicate the mean grain yield (GY; kg ha-1) performance of breeding lines across seasons.

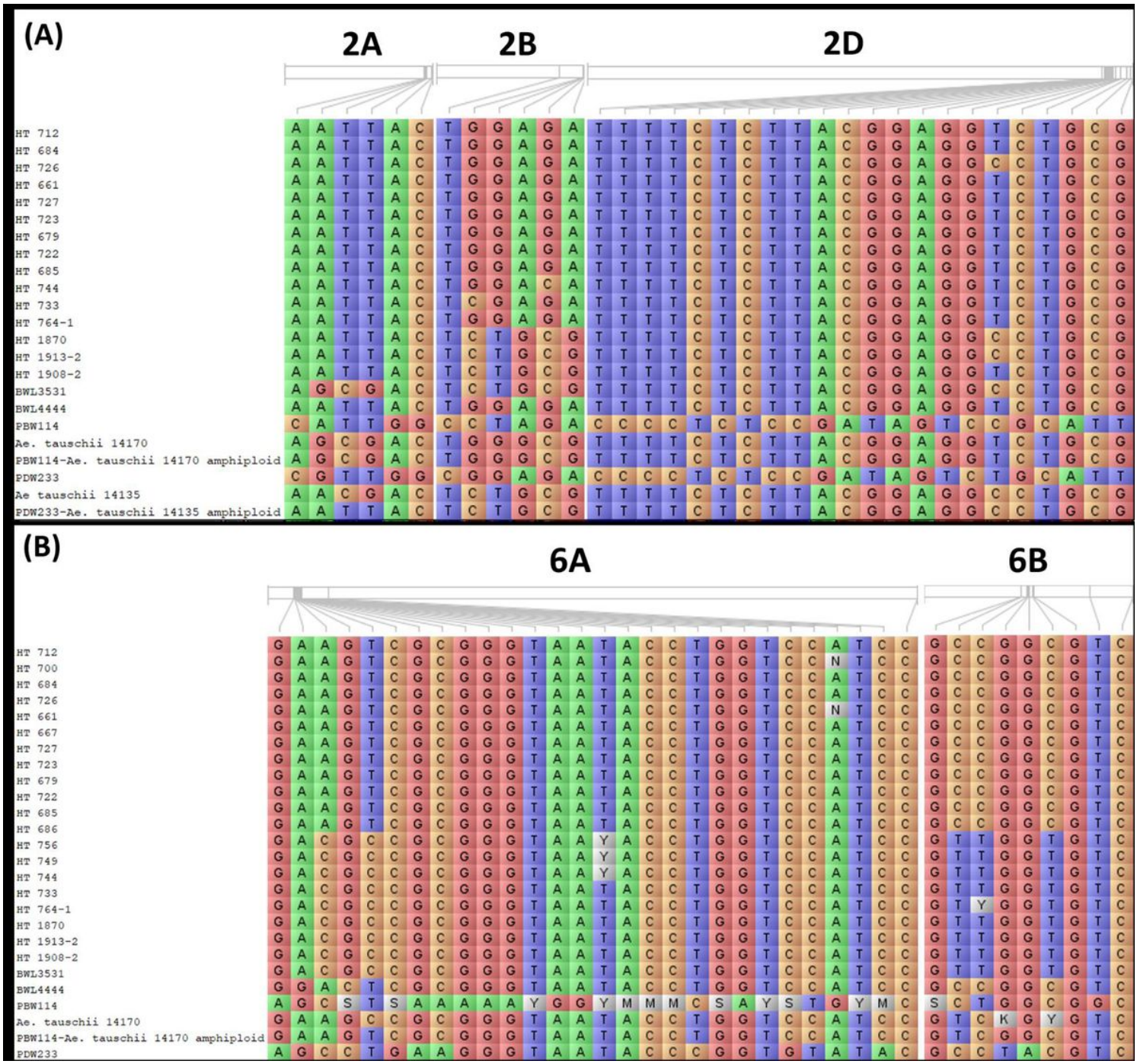

Figure 8

The allelic constitution of the selected promising breeding lines, wild accessions of Ae. tauschii, cultivated and synthetic wheats for the (A) root related traits and (B) grain yield

Supplementary Files

This is a list of supplementary files associated with this preprint. Click to download.

- SupplementaryTablesandFigures01062021.xlsx